CHAPTER III

RESULTS AND DISCUSSION

The aim of the present research was to seek for natural antioxidants from the rhizomes of Waan Ma Lueang (*Curcuma* spp.) that were selected from the primary screening test. Furthermore, this research also aimed to determine the antioxidant activity including DPPH radical scavenging activity, xanthine oxidase-related activity (superoxide scavenging activity and inhibitory effect on xanthine oxidase), and lipid peroxidation inhibitory activity of associated antioxidative compounds.

3.1 Primary screening test of antioxidant activity from some plants in Zingiberaceae family

Eight plants from Zingiberaceae were selected for primary screening test of antioxidant activity based on DPPH radical scavenging. The DPPH method is one of the most effective procedures to estimate the amount of radical trapping materials in the extracts. The dried rhizomes of these plants were extracted successively with dichloromethane, ethyl acetate, and methanol, respectively. The results of DPPH radical scavenging activity were shown in Table 3.1.

From the comparison of the values, the extracts of Waan Ma Lueang (*Curcuma* spp.) showed potent radical trapping activity (IC_{50} = 241.5 ppm for CH_2Cl_2 crude extract and 204.7 ppm for EtOAc crude extract. Its activity was stronger than that of the other plants. Hence, Waan Ma Lueang (*Curcuma* spp.) was selected for further isolation and purification.

Table 3.1 Antioxidant activity of 8 Zingiberaceae plants against the DPPH radical scavenging activity assay

Plant	Solvent	DPPH radical scavenging activity	
		TLC autographic	IC_{50} (ppm)
Boesenbergia pandurata Roxb.	CH_2Cl_2	+	>1000
	EtOAc	+	>1000
	MeOH	-	ND
Zingiber zerumbet Smith.	CH_2Cl_2	+	>1000
	EtOAc	+	>1000
	MeOH	-	ND
Waan En Lueang (*Curcuma* spp.)	CH_2Cl_2	++	449.1
	EtOAc	+++	294.7
	MeOH	+	>1000
Waan Ma Lueang (*Curcuma* spp.)	CH_2Cl_2	+++	241.5
	EtOAc	+++	204.7
	MeOH	+	>1000
Curcuma zedoaria Rose.	CH_2Cl_2	+++	366.5
	EtOAc	++	478.3
	MeOH	+	>1000
Curcuma aeruginosa Roxb.	CH_2Cl_2	+	830.4
	EtOAc	+	>1000
	MeOH	-	ND
Waan Ron Thong (*Globba* spp.)	CH_2Cl_2	++	610.9
	EtOAc	+	>1000
	MeOH	-	ND
Kaempferia galanga Linn.	CH_2Cl_2	+	>1000
	EtOAc	-	ND
	MeOH	-	ND

Note: +++ = Strong activity ND = Not determined

++ = Moderate activity

+ = Weak activity

- = No activity

3.2 The antioxidant activity of various crude extracts from Waan Ma Lueang

Based on DPPH radical scavenging, the dried rhizomes of Waan Ma Lueang (*Curcuma* spp.) were extracted again with various solvents depending on their polarity. Preliminary bioassay was carried out on all extracts to determine the presence of antioxidant activity against DPPH radical scavenging activity, xanthine oxidase-related activity, and lipid peroxidation inhibitory activity using ferric thiocyanate (FTC) assays. The antioxidant activity results of these crude extracts were summarized in Table 3.2.

Table 3.2 Antioxidant activity of various crude extracts

Crude extracts	IC_{50} (ppm)			
	DPPH Assay	Xanthine Oxidase (XOD) Assay		FTC Assay
		Scavenging of $O_2^{-\cdot}$ by XOD	Inhibition of XOD	
Hexane	>1000	>500	>1000	>500
Dichloromethane	241.5	120.1	238.3	128.8
Ethyl acetate	204.7	171.1	191.9	159.9
Methanol	>1000	>500	645.1	>500
BHA	10.2	35.7	-	16.3
Allopurinol	-	-	33.6	-

According to the results of antioxidant activity from various crude extracts, the extracts of dichloromethane and ethyl acetate showed effective activity against all assays. While the hexane crude extract did not give antioxidant activity and the methanol crude extract displayed weak activity. Consequently, dichloromethane and ethyl acetate crude extracts were chosen for further isolation and purification.

3.3 Properties and Structural Elucidation of Isolated Compounds

3.3.1 Structural elucidation of Compound 1

Compound **1** was obtained as bright yellow powder (75.1 mg) from dichloromethane (62.3 mg, 7.8×10^{-2} % w/w) and ethyl acetate (12.8 mg, 4.9×10^{-2} % w/w) crude extracts. Its melting point was 162-164°C and R_f value was 0.50 (SiO_2, 1:19 MeOH/$CHCl_3$).

The IR spectrum (**Figure 3.4**) exhibited the absorption band of hydroxy group (OH) at ν_{max} 3500-2500 cm^{-1} and α,β-unsaturated ketone at ν_{max} 1626 cm^{-1}. Besides, the characteristic absorption peak due to an aromatic moiety was observed at 1602, 1505, and 1431 cm^{-1}.

The mass spectrum of compound **1** (**Figure 3.5**) showed a molecular ion peak, [M^+], at m/z 368 along with fragment ion peak at m/z 137, 150, 177, 191, and 219 in the electron impact mass spectrum (EIMS) (**Scheme 3.1**).

The ^1H NMR spectrum (acetone-d_6) was shown in Figure 3.6. The spectrum indicated one methine proton at δ 5.96 (1H, s) and four trans olefinic protons at δ 6.70 (2H, d, *J*=15.9 Hz) and δ 7.57 (2H, d, *J*=15.9 Hz). It also showed six aromatic protons in a 1,3,4-trisubstitution pattern at δ 6.87 (2H, d, *J*=8.2 Hz), δ 7.17 (2H, dd, *J*=2, 8.2 Hz), and δ 7.33 (2H, d, *J*=1.8 Hz). Moreover, two methoxy groups were observed at δ 3.91 (3H, s) and two hydroxy at δ 8.20 (2H, s).

The ^{13}C NMR spectrum (acetone-d_6) (**Figure 3.8**) demonstrated twenty-one carbons and two substituent groups. Compound **1** had two methoxy carbons at δ 56.3, eleven methine carbons at δ 101.6 (C-1), δ 111.5 (C-6, 6′), δ 116.2 (C-9, 9′), δ 122.2 (C-3, 3′), δ 128.1 (C-10, 10′), and δ 141.4 (C-4, 4′), six quaternary carbons at δ 123.8 (C-5, 5′), δ 148.8 (C-8, 8′), and δ 150.0 (C-7, 7′) and finally a ketone group at δ 185.0. However, the deuterated solvent (acetone-d_6) which was used in the NMR experiment may affected the tautermerization at C-2, 2′ position. From EIMS, ^1H and ^{13}C NMR data, compound **1** was determined as $C_{21}H_{20}O_6$, indicating 12 degrees of unsaturation.

All of the above data suggested the possibility of compound **1** being curcuminoid type. Compound **1** was likely to be 1,7-bis(4-hydroxy-3-methoxyphenyl)-1,6-heptadiene-3-oxo-5-ol or curcumin (**Figure 3.3**). Therefore, the ^1H and ^{13}C chemical shifts of compound **1** were compared to those of reported NMR data of curcumin (Guddadarangvvanahally *et.al.*, 2002). (**Table 3.3, 3.4**) The

complete assignments of ^{1}H and ^{13}C NMR of compound **1** were revealed in Figure 3.1 and 3.2.

Table 3.3 ^{1}H NMR Spectral Data of Curcumin ($CDCl_3$) and Compound **1** (CD_3COOCD_3)

Position of Proton	Chemical shift (ppm)		
	Curcumin ($CDCl_3$)	Compound **1** ($CDCl_3$)	Compound **1** (CD_3COOCD_3)
1	6.06 (s)	5.78 (s)	5.96 (s)
2-OH	16.41 (bs)	16.00 (bs)	-
3, 3′	7.57 (d, *J*=16 Hz)	7.57 (d, *J*=15.9 Hz)	7.57 (d, *J*=15.9 Hz)
4, 4′	6.75 (d, *J*=16 Hz)	6.46 (d, *J*=15.9 Hz)	6.70 (d, *J*=15.9 Hz)
6, 6′	7.32 (d, *J*=2 Hz)	7.03 (d, *J*=2 Hz)	7.33 (d, *J*=1.8 Hz)
7, 7′	-	-	-
8, 8′-OH	9.64 (s)	9.80 (s)	8.20 (s)
9, 9′	6.85 (d, *J*=8.1 Hz)	6.92 (d, *J*=8.2 Hz)	6.87 (d, *J*=8.2 Hz)
10, 10′	7.16 (dd, *J*=2, 8.1 Hz)	7.10 (dd, *J*=1.8, 8.5 Hz)	7.17 (dd, *J*=2, 8.2 Hz)
OMe	3.85 (3H, s)	3.93 (3H, s)	3.91 (3H, s)

Table 3.4 ^{13}C NMR Spectral Data of Curcumin ($CDCl_3$) and Compound **1** (CD_3COOCD_3)

Position of Carbon	Chemical shift (ppm)		
	Curcumin ($CDCl_3$)	Compound **1** ($CDCl_3$)	Compound **1** (CD_3COOCD_3)
1	100.8	101.2	101.6
2, 2′	183.2	183.3	185.0
3, 3′	121.1	121.7	122.2
4, 4′	140.7	140.5	141.4
5, 5′	126.4	127.7	123.8
6, 6′	111.5	109.6	111.5
7, 7′	149.4	147.8	150.0
8, 8′	148.0	146.8	148.8
9, 9′	115.8	114.8	116.2
10, 10′	123.0	122.9	128.1
OMe	55.7	55.9	56.3

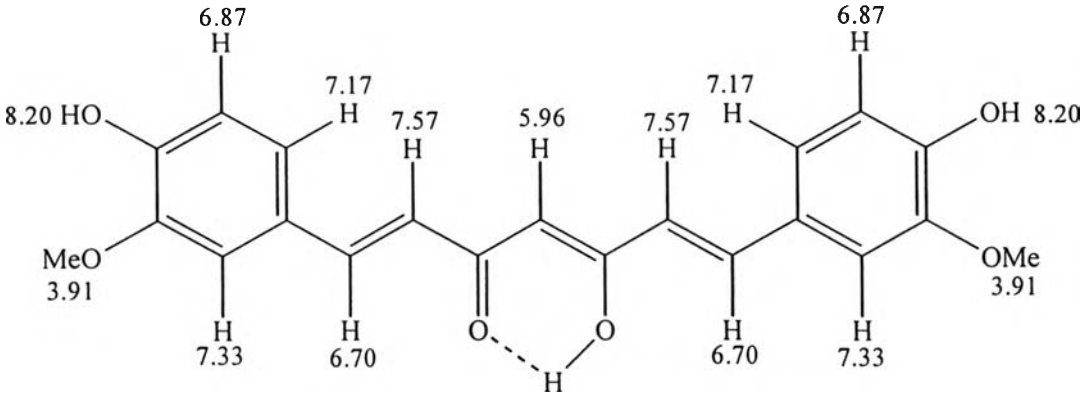

Figure 3.1 The complete assignment of ^{1}H NMR of Compound **1**

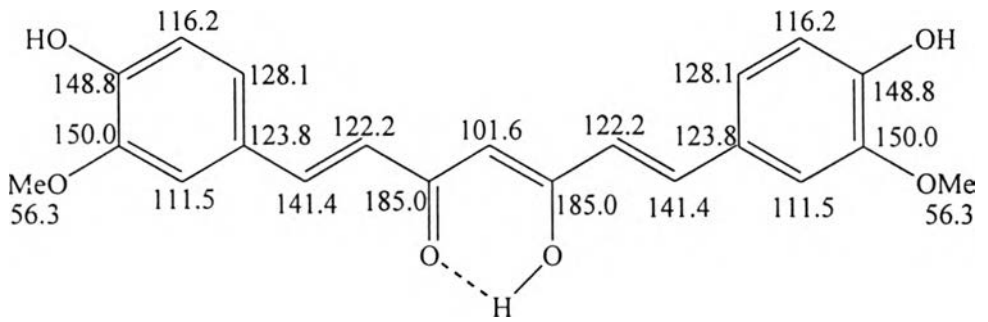

Figure 3.2 The complete assignment of ^{13}C NMR of Compound **1**

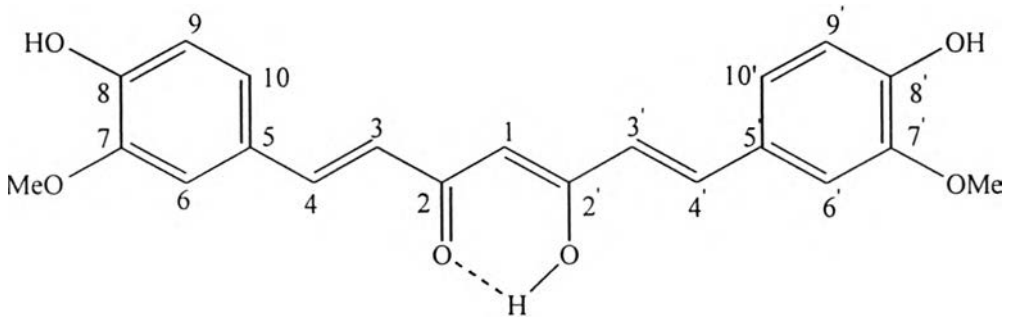

Figure 3.3 The structure of Compound **1** (Curcumin)

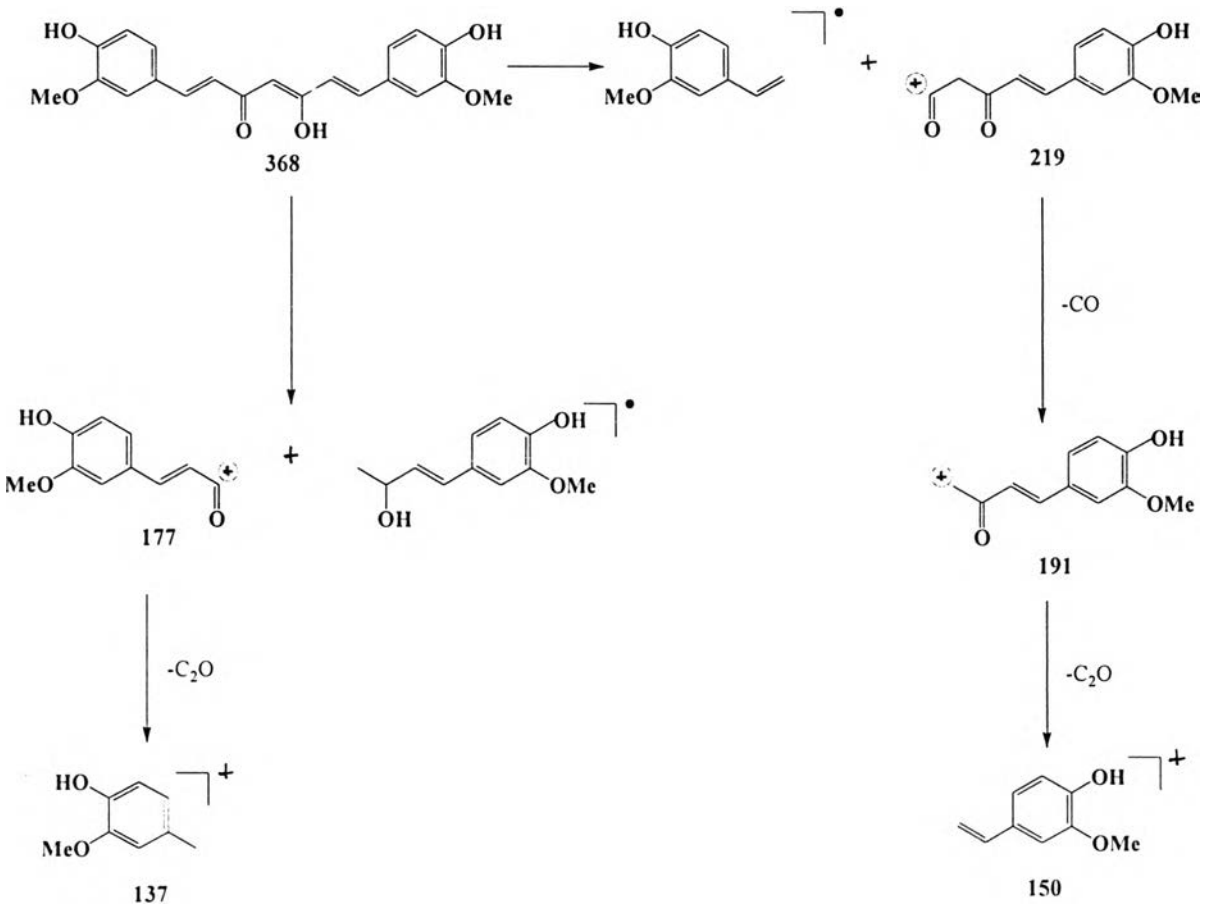

Scheme 3.1 The possible mass fragmentation pattern of Compound **1**

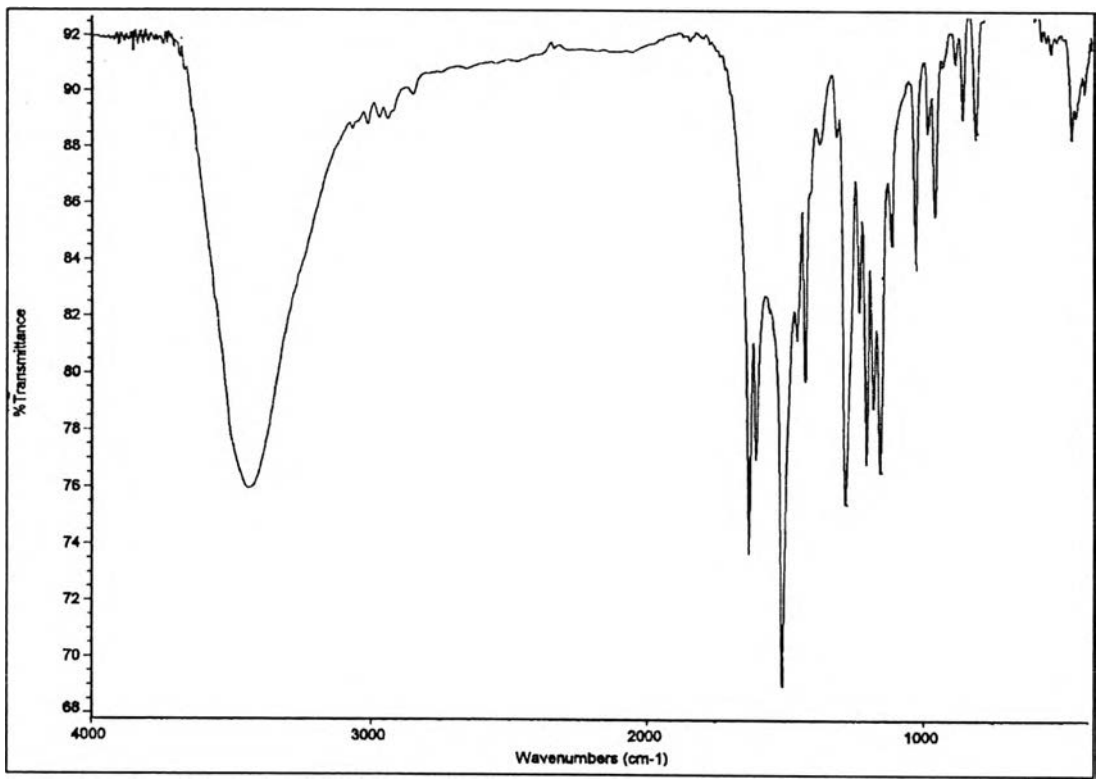

Figure 3.4 The IR spectrum of Compound **1**

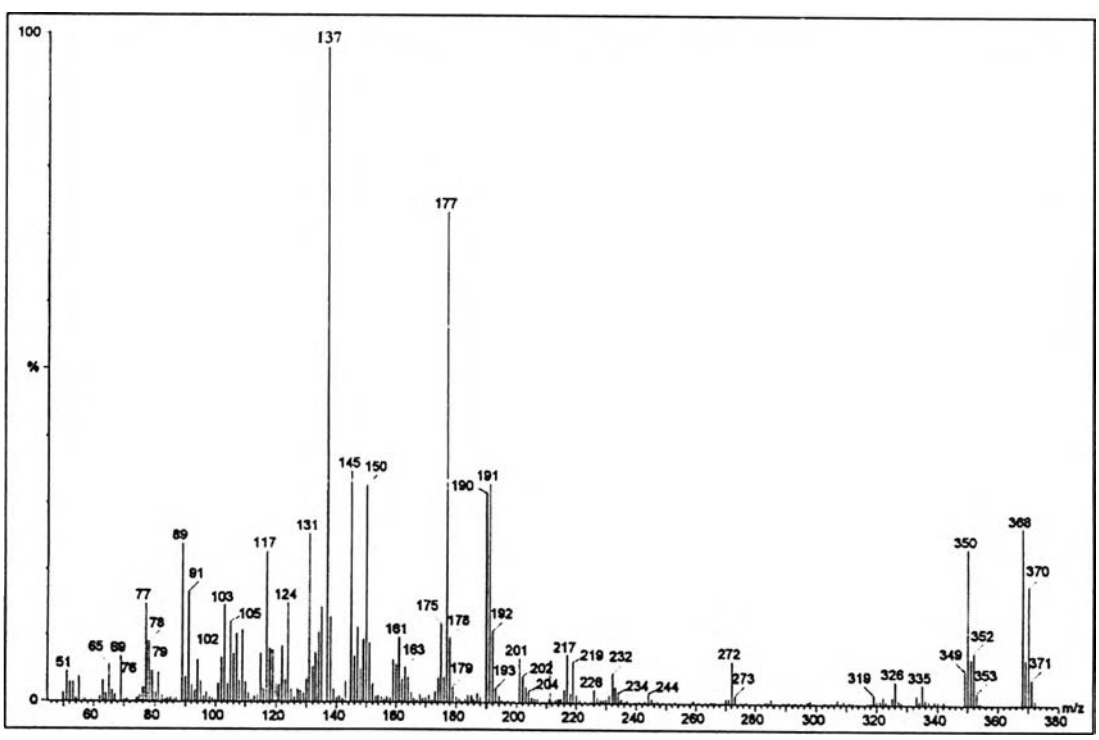

Figure 3.5 The mass spectrum of Compound **1**

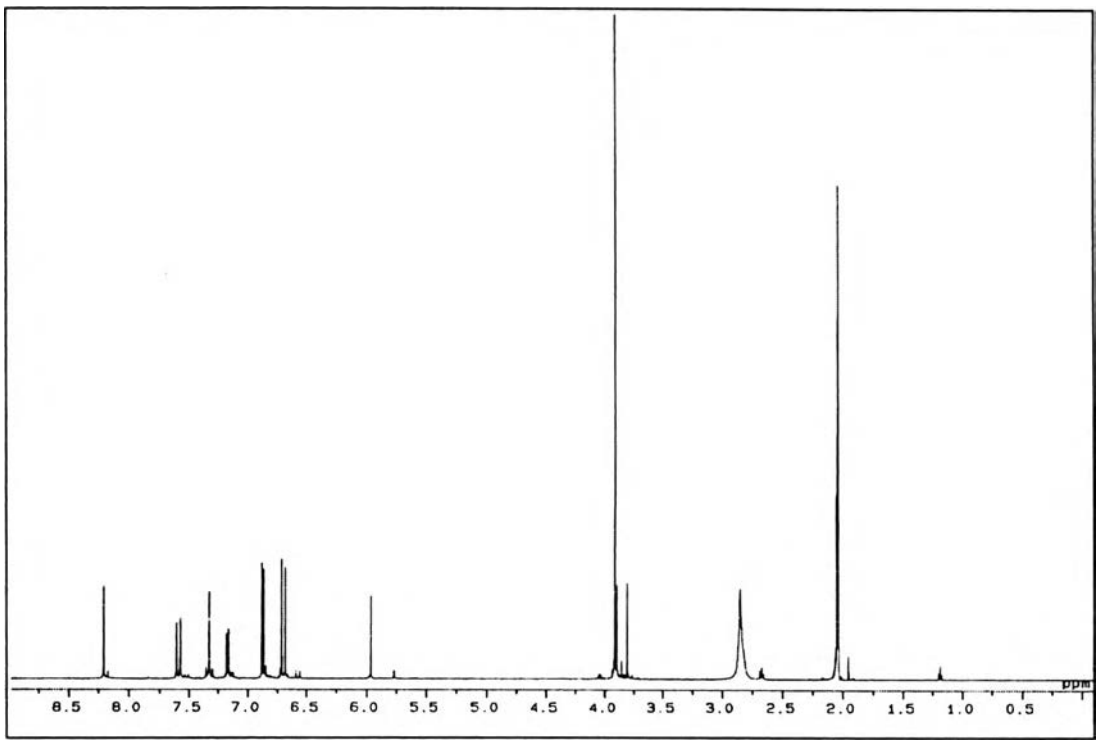

Figure 3.6 The ^{1}H NMR spectrum (CD_3COOCD_3) of Compound **1**

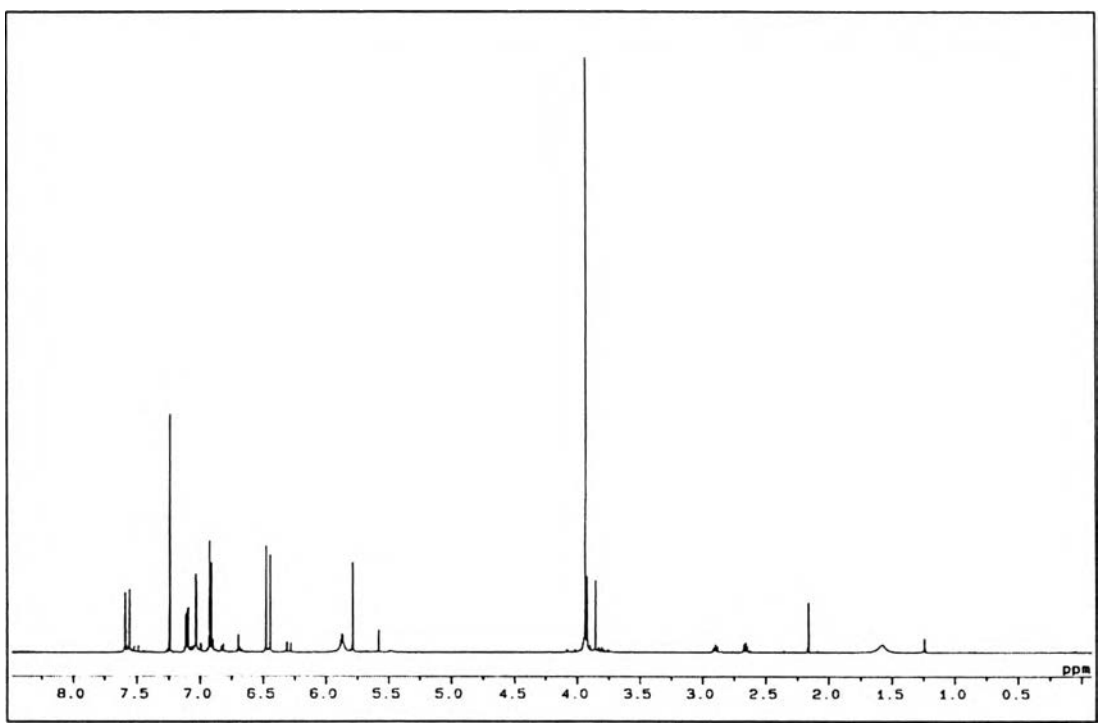

Figure 3.7 The ^{1}H NMR spectrum ($CDCl_3$) of Compound **1**

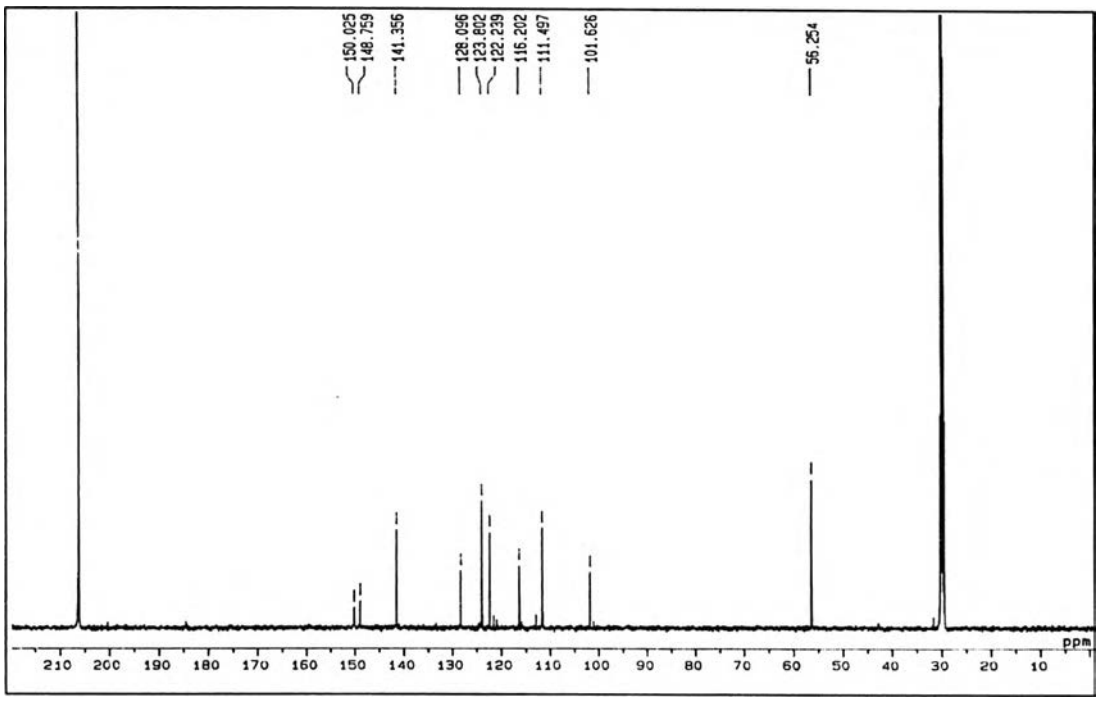

Figure 3.8 The ^{13}C NMR spectrum (CD_3COOCD_3) of Compound **1**

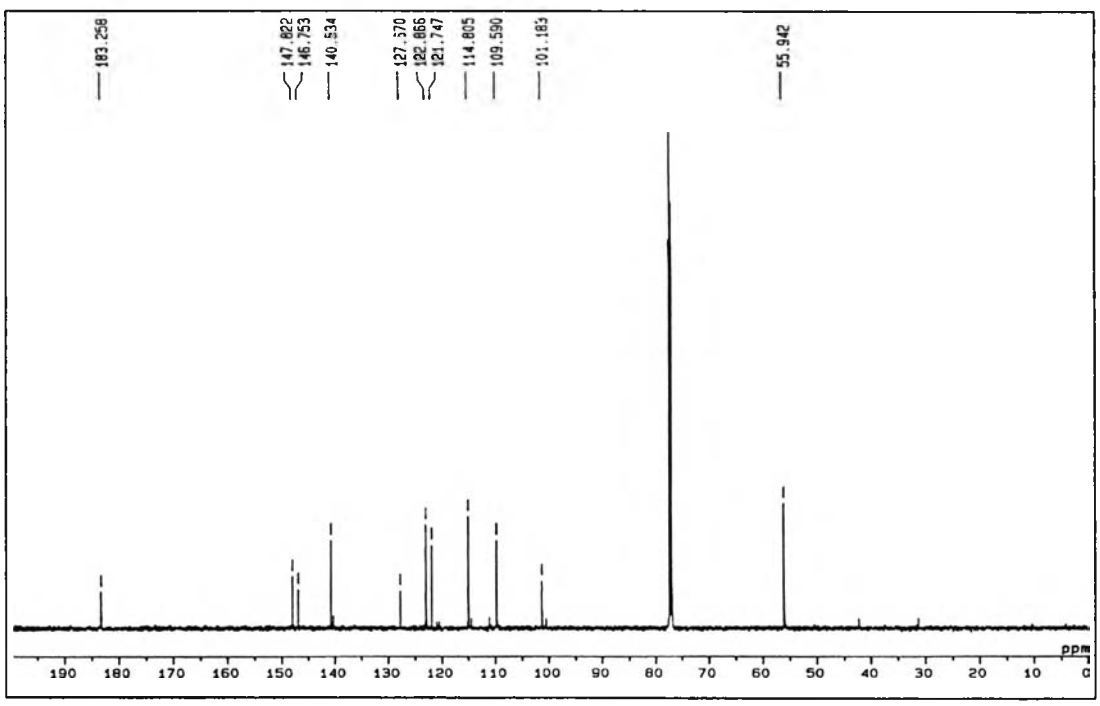

Figure 3.9 The ^{13}C NMR spectrum ($CDCl_3$) of Compound **1**

3.3.2 Structural elucidation of Compound 2

Compound **2**, a yellow powder (50.2 mg) with a melting point 155-157°C, was isolated from dichloromethane (44.0 mg, 5.5 × 10^{-2} % w/w) and ethyl acetate (6.2 mg, 2.4 × 10^{-2} % w/w) crude extracts. Its R_f value was 0.45 (SiO_2, 1:19 MeOH/$CHCl_3$).

Its IR spectrum (**Figure 3.13**) indicated the characteristic OH stretching absorption band of hydroxyl group at ν_{max} 3500-2500 cm^{-1}. The absorption bands of α,β-unsaturated ketone was observed at ν_{max} 1571 cm^{-1}. Additionally, the absorption bands at ν_{max} 1509, 1435, and 1260 cm^{-1}, which were signals of an aromatic moiety, were also observed.

Molecular ion peak (**Figure 3.14**) at m/z 338 corresponded to a molecular formula $C_{20}H_{18}O_5$, indicating 12 degrees of unsaturation. The main fragmentation patterns of compound **3** showed at m/z 91, 119, 147, 177, 191, and 219 (**Scheme 3.2**).

The ^1H NMR spectrum of compound **2** (**Figure 3.15**) revealed one methine proton at δ 5.97 (1H, s) and four trans olefinic protons at δ 6.66 (1H, d, *J*=15.9 Hz), δ 6.71 (1H, d, *J*=15.9 Hz), and δ 7.59 (2H, dd, *J*=15.6, 15.9 Hz). As for aromatic protons, they were observed seven signals at δ 6.87 (1H, d, *J*=7.9 Hz), δ 6.89 (2H, d, *J*=8.5 Hz), δ 7.17 (1H, dd, *J*=1.8, 8.2 Hz), δ 7.33 (1H, d, *J*=1.8 Hz), and δ 7.56 (2H, d, *J*=8.6 Hz). Furthermore, compound **2** had one methoxy group at δ 3.91 (3H,s).

The ^{13}C NMR spectrum of compound **2** (**Figure 3.16**) indicated fifteen signals of eighteen carbons. The spectrum revealed the presence of one methoxy carbon at δ 56.3, twelve methine carbons at δ 101.7 (C-1), δ 111.4 (C-6′), δ 116.2 (C-9′), δ 116.7 (C-7, 9), δ 122.0 (C-3), δ 122.2 (C-3′), δ 123.9 (C-10′), δ 130.9 (C-6, 10), δ 141.0 (C-4), and δ 141.3 (C-4′). Besides, compound **2** had five quaternary carbons at δ 127.6 (C-5), δ 128.1 (C-5′), δ 130.9 (C-8′), δ 148.8 (C-7′), and δ 160.5 (C-8). Therefore, the ^1H and ^{13}C NMR of this compound showed the spectra similar to those of compound **1**. We were able to resolve the structure by comparing ^1H and ^{13}C NMR data of this compound with compound **1** as well as with the literature data (Guddadarangvvanahally *et.al.*, 2002).

Based on all of the above spectroscopic data, compound **2** was assigned as 1-(4-hydroxyphenyl)-7-(4-hydroxy-3-methoxyphenyl)-1,6-heptadiene-3-oxo-5-ol or demethoxycurcumin (**Figure 3.12**). Thus, the assignment of ^{1}H and ^{13}C NMR (**Table 3.5, 3.6**) was achieved by comparison with those of proclaimed compound (Guddadarangvvanahally *et.al.*, 2002). The absolute assignments of ^{1}H and ^{13}C NMR of compound **2** were shown in Figure 3.10 and 3.11.

Table 3.5 ^{1}H NMR Spectral Data of Demethoxycurcumin ($CDCl_3$) and Compound **2** (CD_3COOCD_3)

Position of proton	Chemical shift (ppm)	
	Demethoxycurcumin ($CDCl_3$)	Compound **2** (CD_3COOCD_3)
1	5.97 (s)	5.97 (s)
2-OH	-	-
3, 3′	7.60 (d, *J*=16 Hz)	7.59 (dd, *J*=15.6, 15.9 Hz)
4, 4′	6.69 (d, *J*=16 Hz) 6.64 (d, *J*=16 Hz)	6.71 (d, *J*=15.9 Hz) 6.66 (d, *J*=15.9 Hz)
6, 6′	6.90 (d, *J*=8 Hz) 7.34 (d, *J*=1.7 Hz)	7.56 (d, *J*=8.6 Hz) 7.33 (d, *J*=1.8 Hz)
7, 7′	7.56 (d, *J*=8 Hz)	6.89 (d, *J*=8.5 Hz)
8, 8′-OH	-	-
9, 9′	7.56 (d, *J*=8.5 Hz) 6.88 (d, *J*=7.9 Hz)	6.89 (d, *J*=8.5 Hz) 6.87 (d, *J*=7.9 Hz)
10, 10′	6.90 (d, *J*=8 Hz) 7.27 (dd, *J*=1.7, 8 Hz)	7.56 (d, *J*=8.6 z) 7.17 (dd, *J*=1.8, 8.2 Hz)
OMe	3.92 (3H, s)	3.91 (3H, s)

Table 3.6 ^{13}C NMR Spectral Data of Demethoxycurcumin ($CDCl_3$) and Compound **2** (CD_3COOCD_3)

Position of carbon	Chemical shift (ppm)	
	Demethoxycurcumin ($CDCl_3$)	Compound **2** (CD_3COOCD_3)
1	101.6	101.7
2, 2′	184.4, 184.5	-
3, 3′	122.1, 122.3	122.0, 122.2
4, 4′	141.0, 141.4	141.0, 141.3
5, 5′	127.7, 128.2	127.6, 128.1
6, 6′	130.9, 111.5	130.9, 111.4
7, 7′	116.8, 148.8	116.7, 148.8
8, 8′	160.5, 150.0	160.5, 130.9
9, 9′	116.8, 116.2	116.7, 116.2
10, 10′	130.9, 123.8	130.9, 123.9
OMe	56.3	56.3

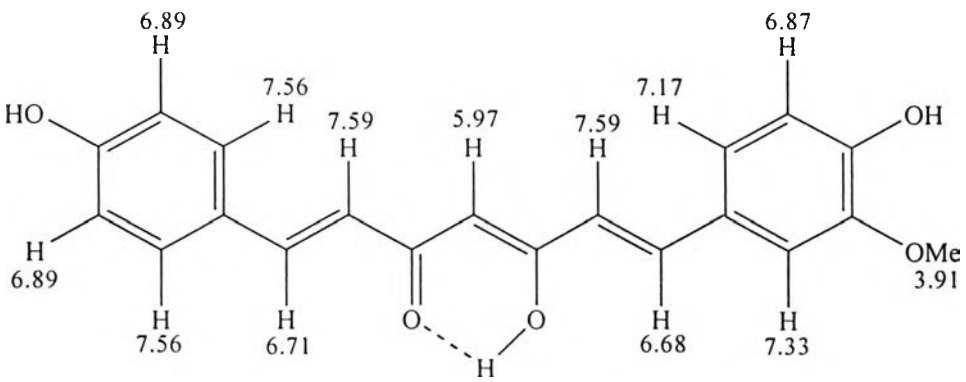

Figure 3.10 The full assignment of ^{1}H NMR of Compound **2**

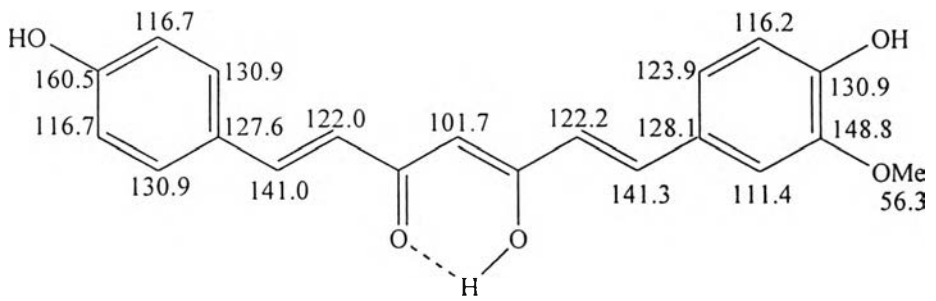

Figure 3.11 The full assignment of ^{13}C NMR of Compound **2**

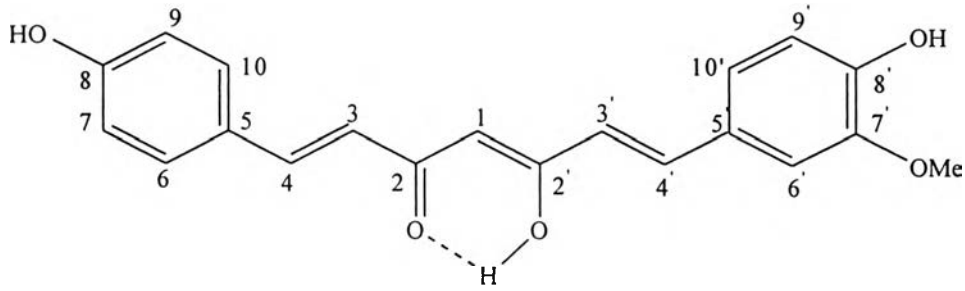

Figure 3.12 The structure of Compound **2** (Demethoxycurcumin)

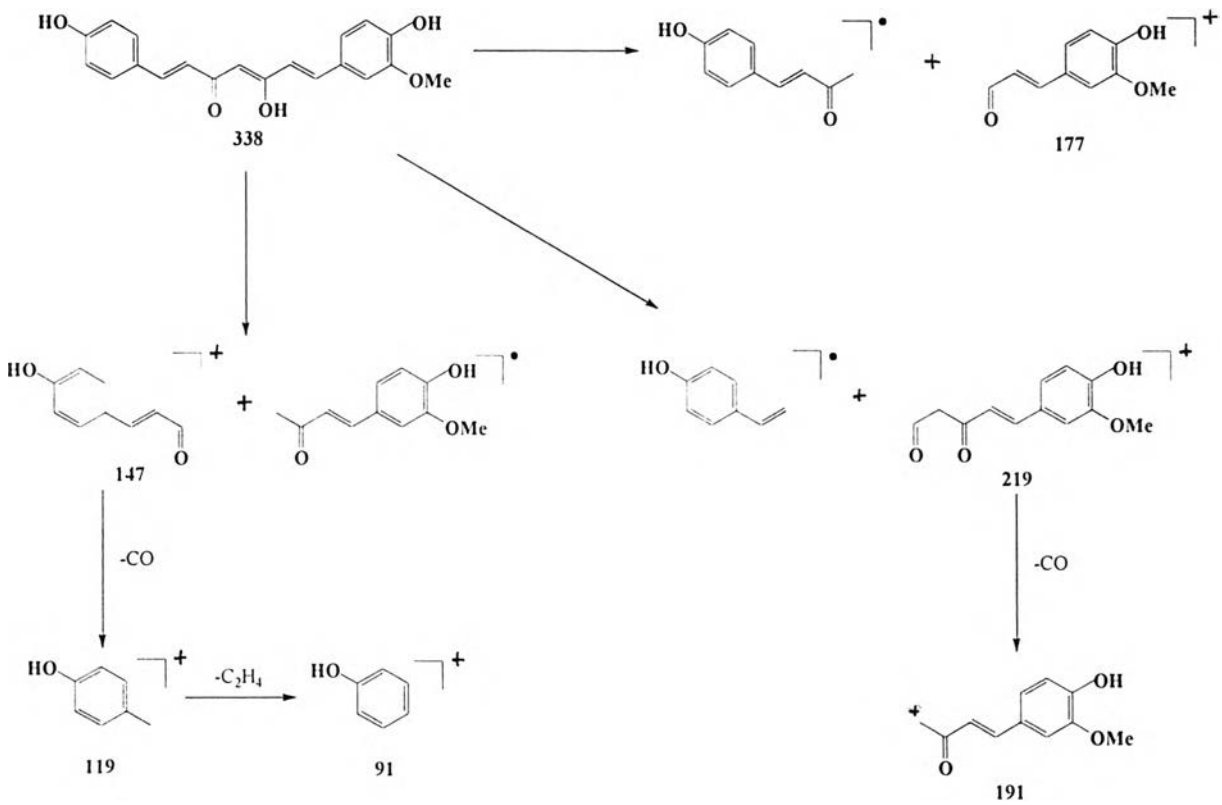

Scheme 3.2 The possible mass fragmentation pattern of Compound **2**

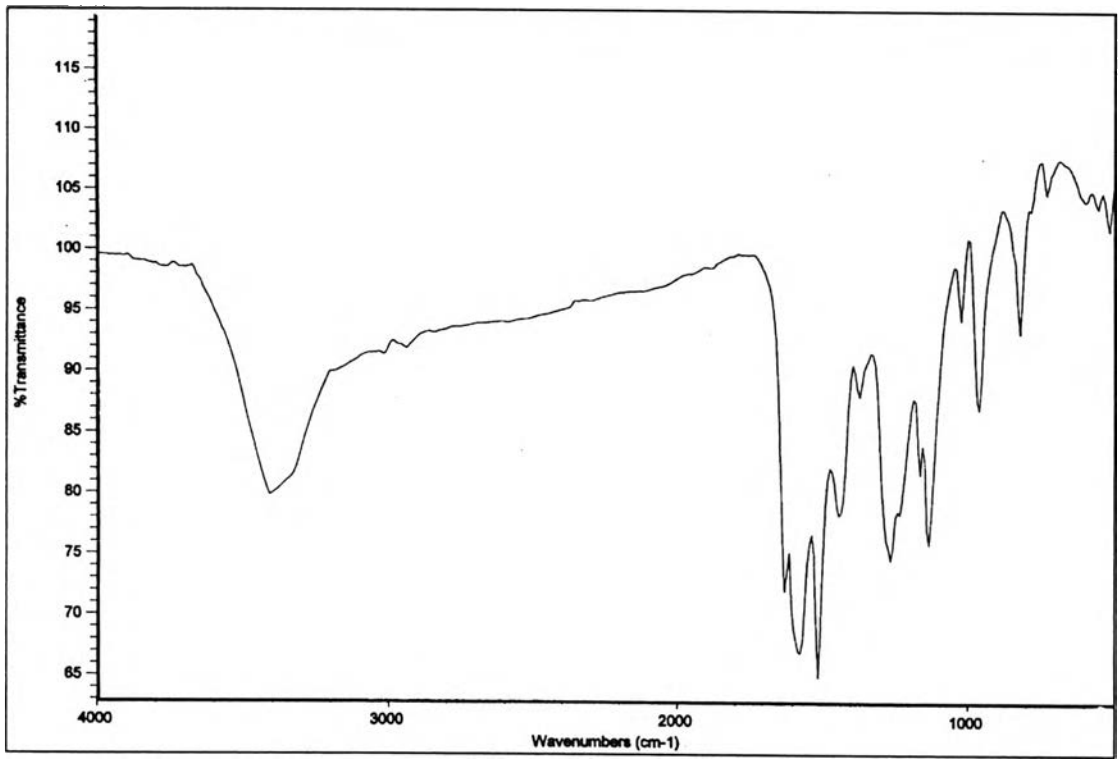

Figure 3.13 The IR spectrum of Compound **2**

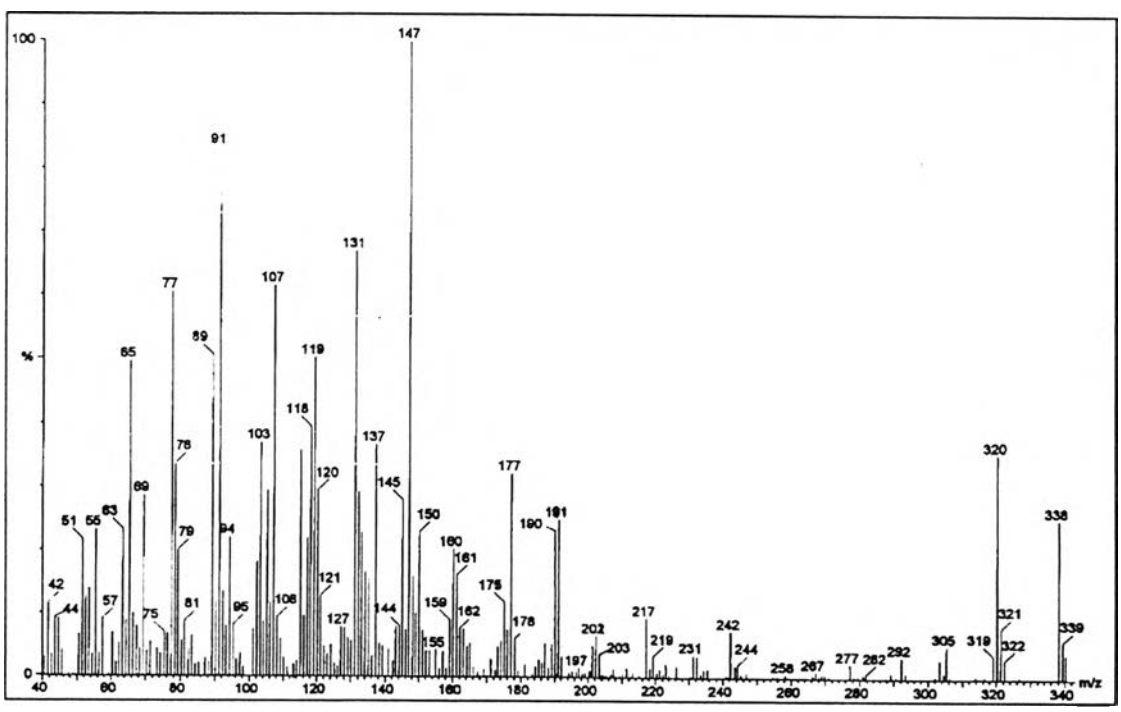

Figure 3.14 The mass spectrum of Compound **2**

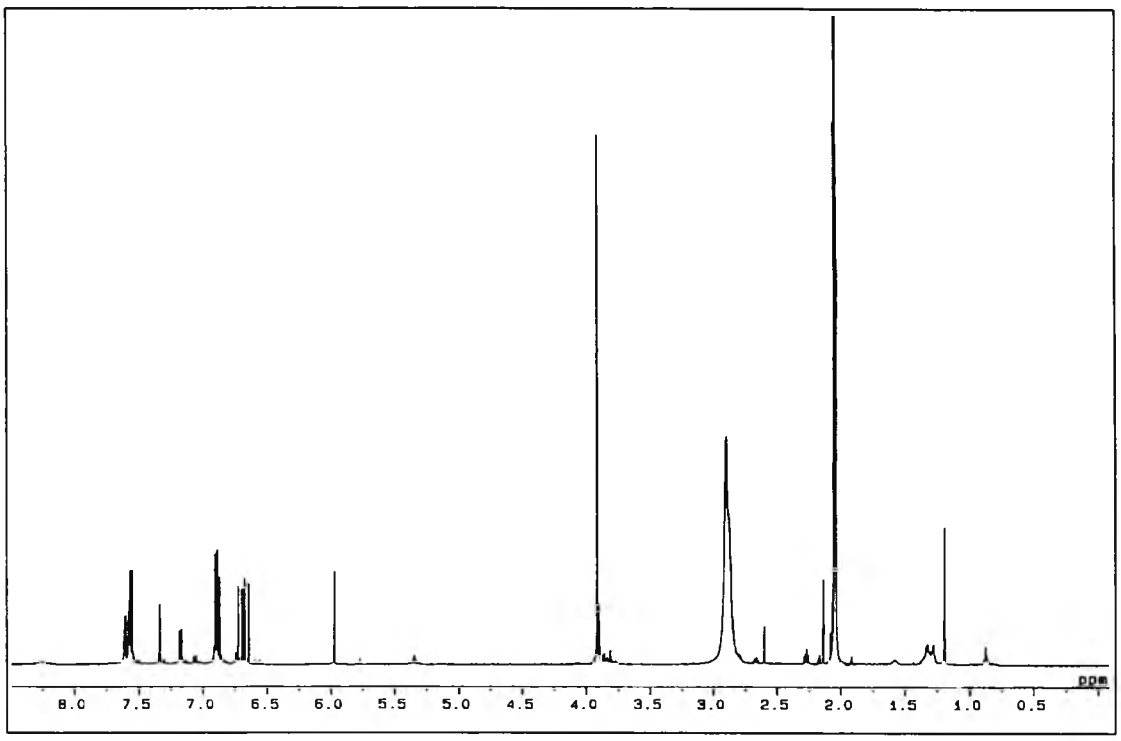

Figure 3.15 The ^{1}H NMR spectrum (CD_3COOCD_3) of Compound **2**

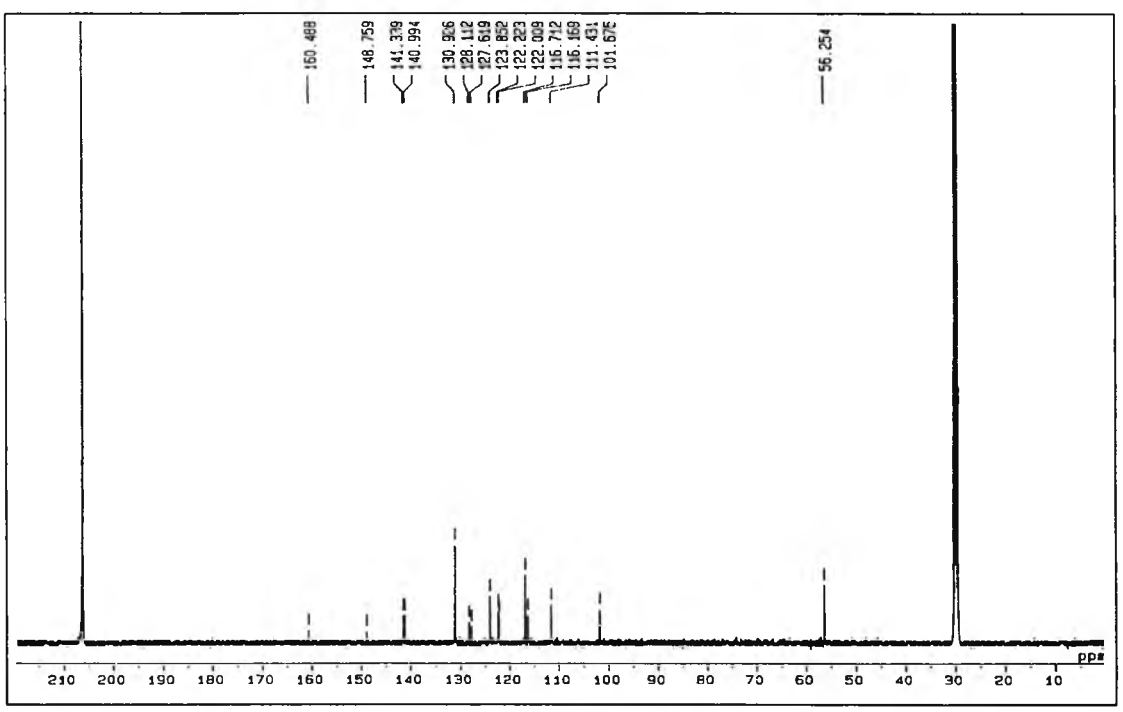

Figure 3.16 The ^{13}C NMR spectrum (CD_3COOCD_3) of Compound **2**

3.3.3 Structural elucidation of Compound 3

Compound **3** (31.6 mg) was isolated from dichloromethane (24.4 mg, 3.0×10^{-2} % w/w) and ethyl acetate (7.2 mg, 2.8×10^{-2} % w/w) crude extracts. It was obtained as bright orange powder with melting point 199-201°C. It had R_f value at 0.35 (SiO_2, 1:19 MeOH/$CHCl_3$).

According to the IR spectrum of compound **3** (**Figure 3.20**), there were absorption bands of hydroxy (OH) at ν_{max} 3500-2500 cm^{-1} and α,β-unsaturated ketone at ν_{max} 1599 cm^{-1}. In addition, it also showed the characteristic of aromatic moiety at ν_{max} 1513, 1443, and 1272 cm^{-1}.

The mass spectrum of compound **3** (**Figure 3.21**) indicated a molecular ion peak at m/z 308. The molecular formula of this compound was assigned as $C_{19}H_{16}O_4$. Moreover, it displayed the principal fragmentation patterns at m/z 91, 119, 147, 161, and 189 (**Scheme 3.3**).

The ^1H NMR spectrum of compound **3** (**Figure 3.22**) showed one methine proton at δ 5.98 (1H,s) and four trans olefinic protons at δ 6.66 (2H, d, *J*=15.9 Hz) and δ 7.60 (2H, d, *J*=15.9 Hz). Additionally, there were eight aromatic protons in a 1,4-disubstitution pattern at δ 6.87 (4H, d, *J*=8.5 Hz) and δ 7.56 (4H, d, *J*=8.5 Hz).

As for the ^{13}C NMR spectrum (**Figure 3.23**), it exhibited nineteen signals. Compound **3** had thirteen methine carbons at δ 101.7 (C-1), δ 116.7 (C-7, 7′, 9, 9′), δ 122.0 (C-3, 3′), δ 130.9 (C-6, 6′, 10, 10′), and δ 141.0 (C-4, 4′). Four quaternary carbons were observed at δ 127.6 (C-5, 5′) and δ 160.5 (C-8, 8′). Besides, it showed the carbonyl group at δ 185.0 (C-2, 2′). The ^1H and ^{13}C NMR spectra of this compound revealed similar to those of compounds **1** and **2**.

From the comparison of all spectroscopic data with published data of bisdemethoxycurcumin (Guddadarangvvanahally *et.al.*, 2002), which were displayed in Table 3.7 and 3.8, compound **3** was elucidated as 1,7-bis(4-hydroxyphenyl)-1,6-heptadiene-3-oxo-5-ol or bisdemethoxycurcumin (**Figure 3.19**). The total assignments of ^1H and ^{13}C NMR of compound **3** were shown in Figure 3.17 and 3.18.

Table 3.7 ^{1}H NMR Spectral Data of Bisdemethoxycurcumin ($CDCl_3$) and Compound **3** (CD_3COOCD_3)

Position of proton	Chemical shift (ppm)	
	Bisdemethoxycurcumin ($CDCl_3$)	Compound **3** (CD_3COOCD_3)
1	6.03 (s)	5.98 (s)
2-OH	16.4 (bs)	-
3, 3′	7.56 (d, *J*=15.9 Hz)	7.60 (d, *J*=15.9 Hz)
4, 4′	7.56 (d, *J*=15.9 Hz)	6.66 (d, *J*=15.9 Hz)
6, 6′	7.56 (d, *J*=8.2 Hz)	7.56 (d, *J*=8.5 Hz)
7, 7′	6.84 (d, *J*=8.2 Hz)	6.87 (d, *J*=8.5 Hz)
8, 8′-OH	10.03 (s)	-
9, 9′	6.84 (d, *J*=8.2 Hz)	6.87 (d, *J*=8.5 Hz)
10, 10′	7.56 (d, *J*=8.2 z)	7.56 (d, *J*=8.5 z)

Table 3.8 ^{13}C NMR Spectral Data of Bisdemethoxycurcumin ($CDCl_3$) and Compound **3** (CD_3COOCD_3)

Position of carbon	Chemical shift (ppm)	
	Bisdemethoxycurcumin ($CDCl_3$)	Compound **3** (CD_3COOCD_3)
1	100.9	101.7
2, 2′	183.2	185.0 (bs)
3, 3′	120.8	122.0
4, 4′	140.3	141.0
5, 5′	125.8	127.6
6, 6′	130.3	130.9
7, 7′	115.9	116.7
8, 8′	159.8	160.5
9, 9′	115.9	116.7
10, 10′	130.3	130.9

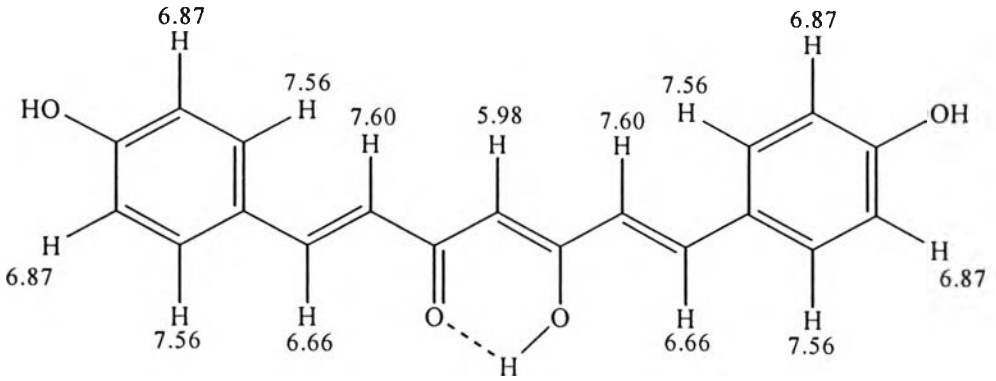

Figure 3.17 The assignment of ^{1}H NMR of Compound **3**

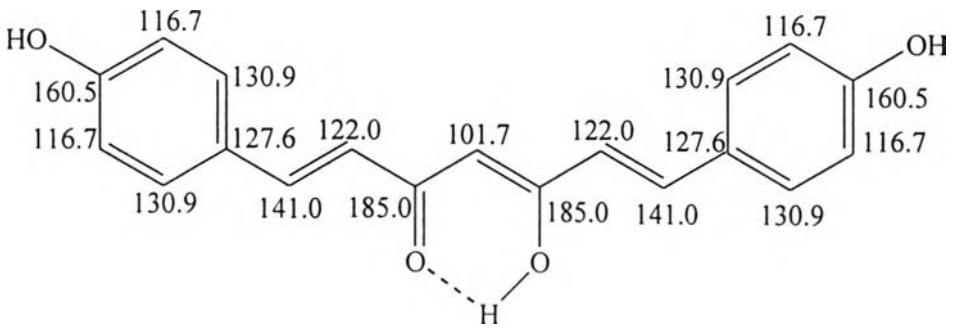

Figure 3.18 The assignment of ^{13}C NMR of Compound **3**

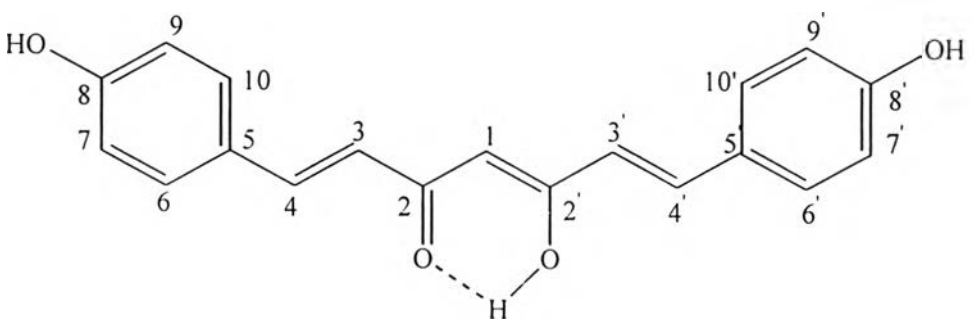

Figure 3.19 The structure of Compound **3** (Bisdemethoxycurcumin)

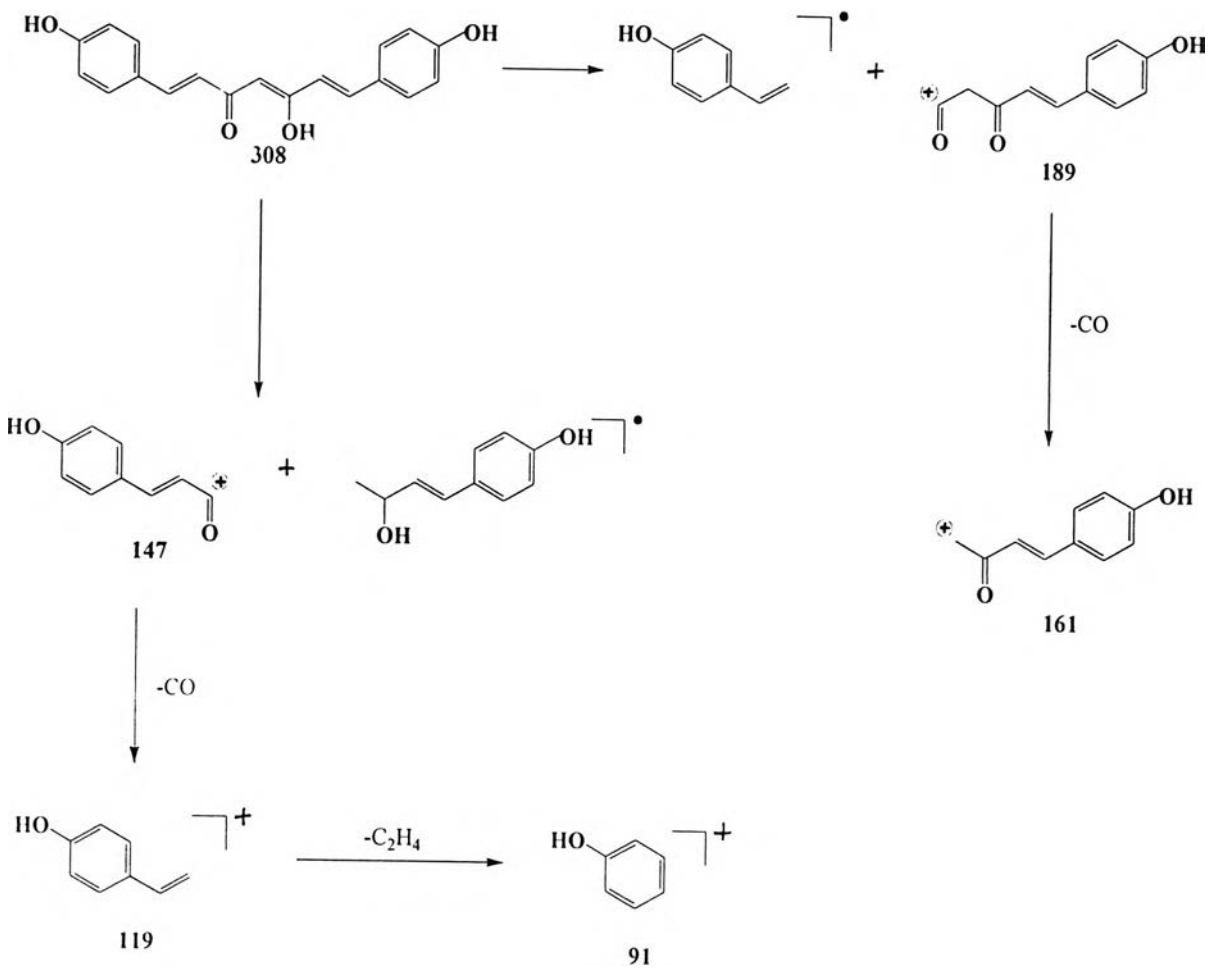

Scheme 3.3 The possible mass fragmentation pattern of Compound **3**

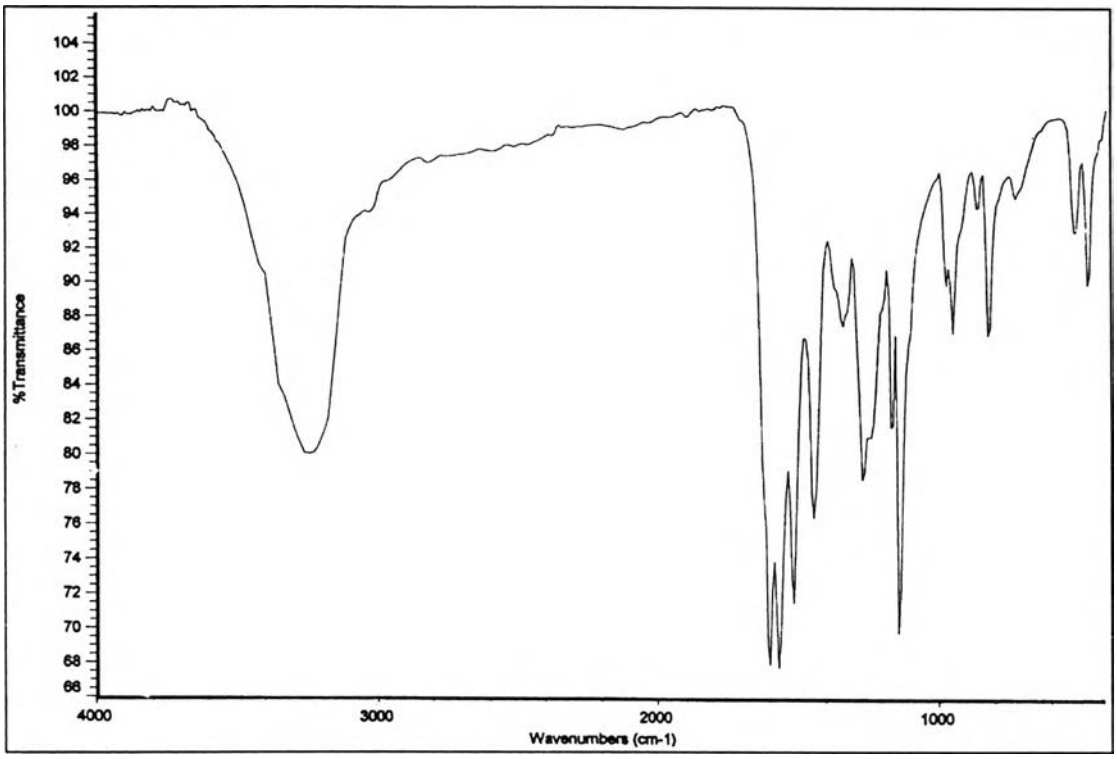

Figure 3.20 The IR spectrum of Compound **3**

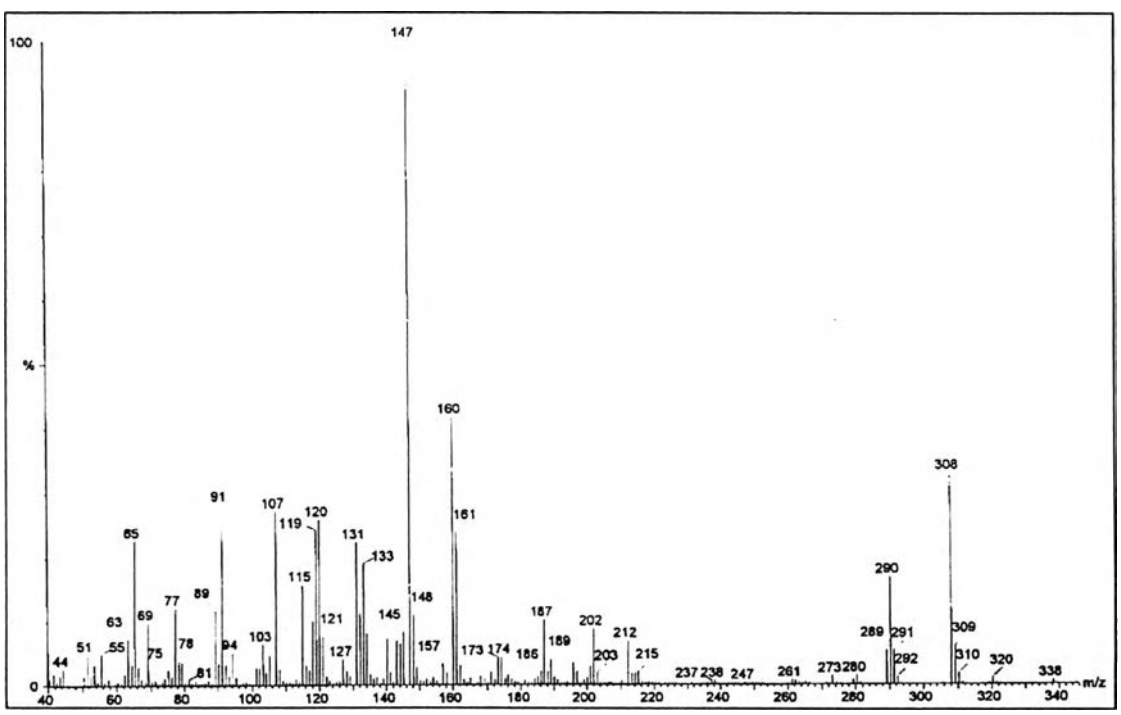

Figure 3.21 The mass spectrum of Compound **3**

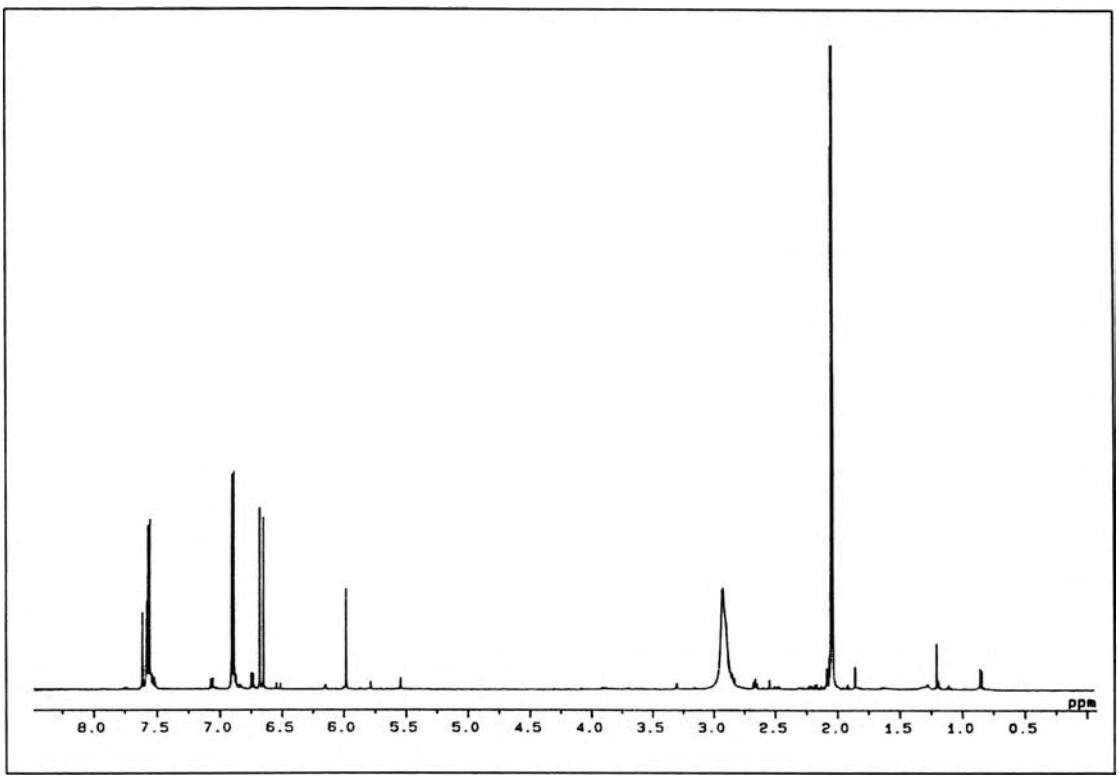

Figure 3.22 The ^{1}H NMR spectrum (CD_3COOCD_3) of Compound **3**

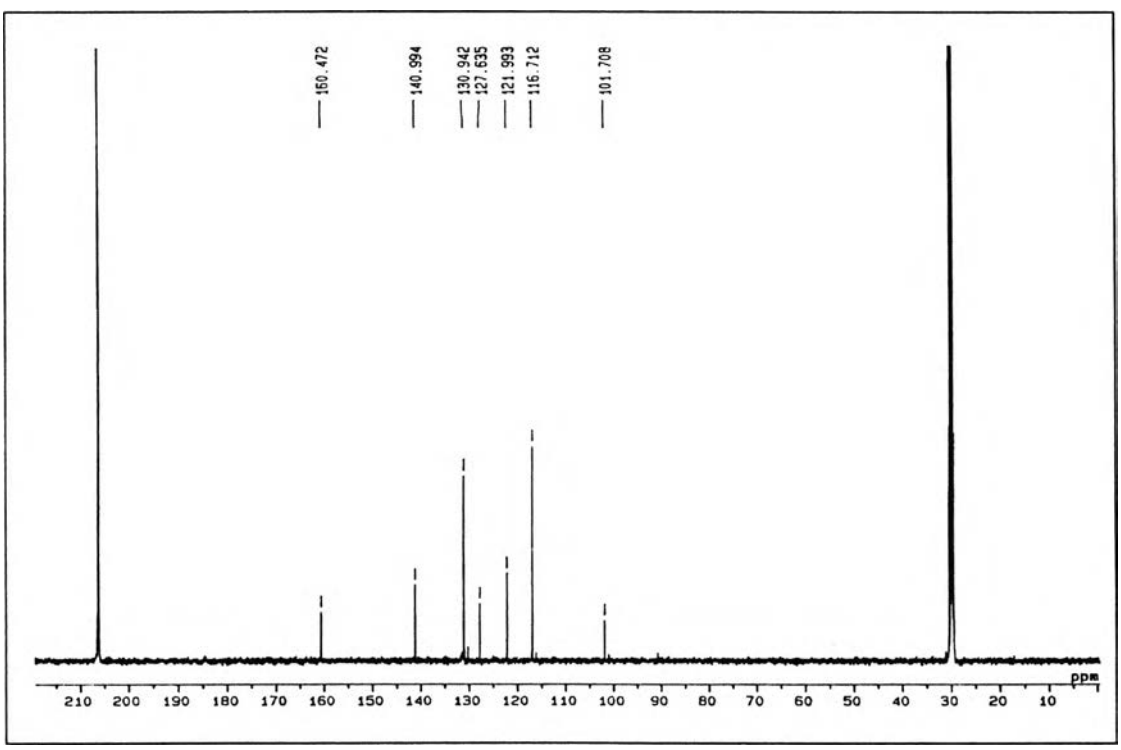

Figure 3.23 The ^{13}C NMR spectrum (CD_3COOCD_3) of Compound **3**

3.3.4 Structural elucidation of Compound 4

Compound **4** (37.8 mg.) was obtained as colorless oil from dichloromethane (20.8 mg, 2.6×10^{-2} % w/w) and ethyl acetate (17.0 mg, 6.5×10^{-2} % w/w) crude extracts. It was purified by chromatotron eluting with 1:9 EtOAc/Hexane. It has R_f value 0.47 (SiO_2, 1:9 EtOAc/CH_2Cl_2).

Its IR spectrum (**Figure 3.27**) displayed the characteristic of aromatic moiety at ν_{max} 3058, 1517, 1442, and 1125 cm^{-1}, CH at ν_{max} 2984 cm^{-1}, C=O and C=C conjugated ketone system at ν_{max} 1689 and 1626 cm^{-1}, and finally, para-substituted aromatic at ν_{max} 895 cm^{-1}.

The EIMS gave a dominant fragment ion peak at m/z 216 (**Figure 3.28**). The molecular formula of compound **4** was determined as $C_{15}H_{20}O$. Its main fragmentation pattern was at m/z 77, 83, 91, 119, 133, and 201 (**Scheme 3.4**).

The ^1H NMR spectrum (**Figure 3.29**) indicated the signals of four aromatic protons at δ 7.12 (4H, d, *J*=8.1 Hz), two methine protons at δ 3.32 (1H, m) and δ 6.05 (1H, m), and one methylene proton at δ 2.70 (2H, m). The signals of methyl group showed at δ 1.27 (3H, d, *J*=7.0 Hz), δ 1.88 (3H, s), δ 2.13 (3H,s), and δ 2.33 (3H,s).

The ^{13}C NMR spectrum (**Figure 3.30**) revealed four methyl carbons at δ 20.7 (C-12), δ 21.0 (C-14), δ 22.0 (C-15), and δ 27.6 (C-13). Six methine carbons were observed at δ 35.3 (C-7), 124.1 (C-10), δ 126.6 (C-3, 5), and δ 129.1 (C-2, 6). It also showed one methylene carbon at δ 52.7 (C-8) and three quarternary carbons at δ 135.5 (C-11), δ 143.7 (C-1), and δ 155.1 (C-4). In addition, one ketone group was recognized at δ 199.9 (C-9). From the DEPT 90 and 135 spectra (**Figure 3.31**), compound **4** contained four quarternary carbons, six methine carbons, one methylene carbon, and four methyl carbons. From the basis of spectroscopic observation, it was deduced to be a sesquiterpene derivative.

In terms of all evidences from spectroscopic data, we suggested that compound **4** was structurally related to 2-methyl-6-(4-methylphenyl)-2-hepten-4-one or *ar*-turmerone (**Figure 3.26**). Consequently, The ^1H NMR data of compound **4** was compared with those of previously published of *ar*-turmerone (Helen *et.al.*, 1982), which was shown in Table 3.9, and the ^{13}C NMR spectral data of this compound was revealed in Table 3.10. The accomplish assignments of ^1H and ^{13}C NMR of compound **4** were displayed in Figure 3.24 and Figure 3.25.

revealed in Table 3.10. The accomplish assignments of ^{1}H and ^{13}C NMR of compound **4** were displayed in Figure 3.24 and Figure 3.25.

Table 3.9 ^{1}H NMR Spectral Data of *ar*-Turmerone and Compound **4**

Position of proton	Chemical shift (ppm)	
	ar-Turmerone ($CDCl_3$)	Compound **4** ($CDCl_3$)
2, 6 – 3,5	7.08 (4H, s)	7.12 (d, *J*=8.1 Hz)
7	5.99 (1H, m)	6.05 (1H, m)
8	2.58 (2H, d, *J*=2 Hz)	2.70 (2H, m)
10	3.10 (1H, m)	3.32 (1H, m)
12	1.18, 1.23 (3H, 2s)	1.27 (3H, d, *J*=7.0 Hz)
13	2.08 (3H, d, *J*=2 Hz)	2.13 (3H, s)
14	1.84 (3H,d, *J*=2 Hz)	1.88 (3H,s)
15	2.29 (3H,s)	2.33 (3H, s)

Table 3.10 ^{13}C NMR Spectral Data of Compound **4**

Position of carbon	Compound **4** ($CDCl_3$)
1	143.7
2, 6	129.1
3, 5	126.6
4	155.1
7	35.3
8	52.7
9	199.9
10	124.1
11	135.5
12	20.7
13	27.6
14	21.0
15	22.0

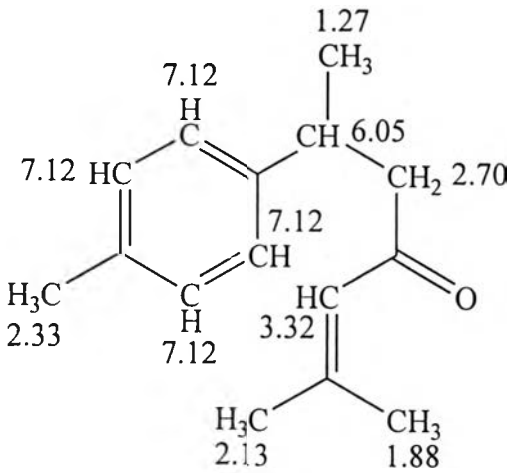

Figure 3.24 The assignment of ^{1}H NMR of Compound **4**

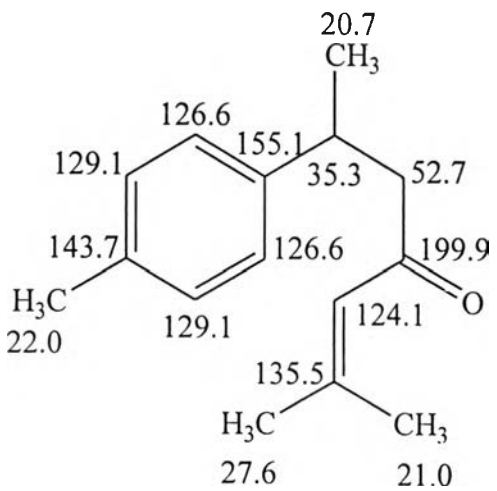

Figure 3.25 The assignment of ^{13}C NMR of Compound **4**

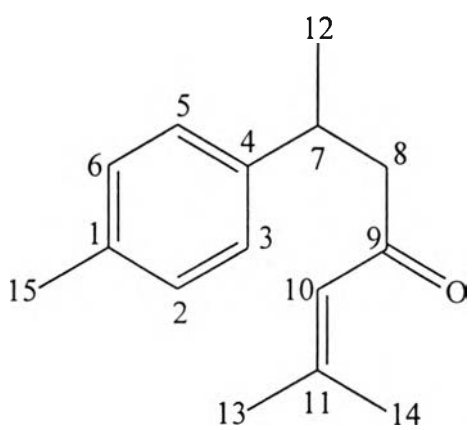

Figure 3.26 The structure of Compound **4** (*ar*-Turmerone)

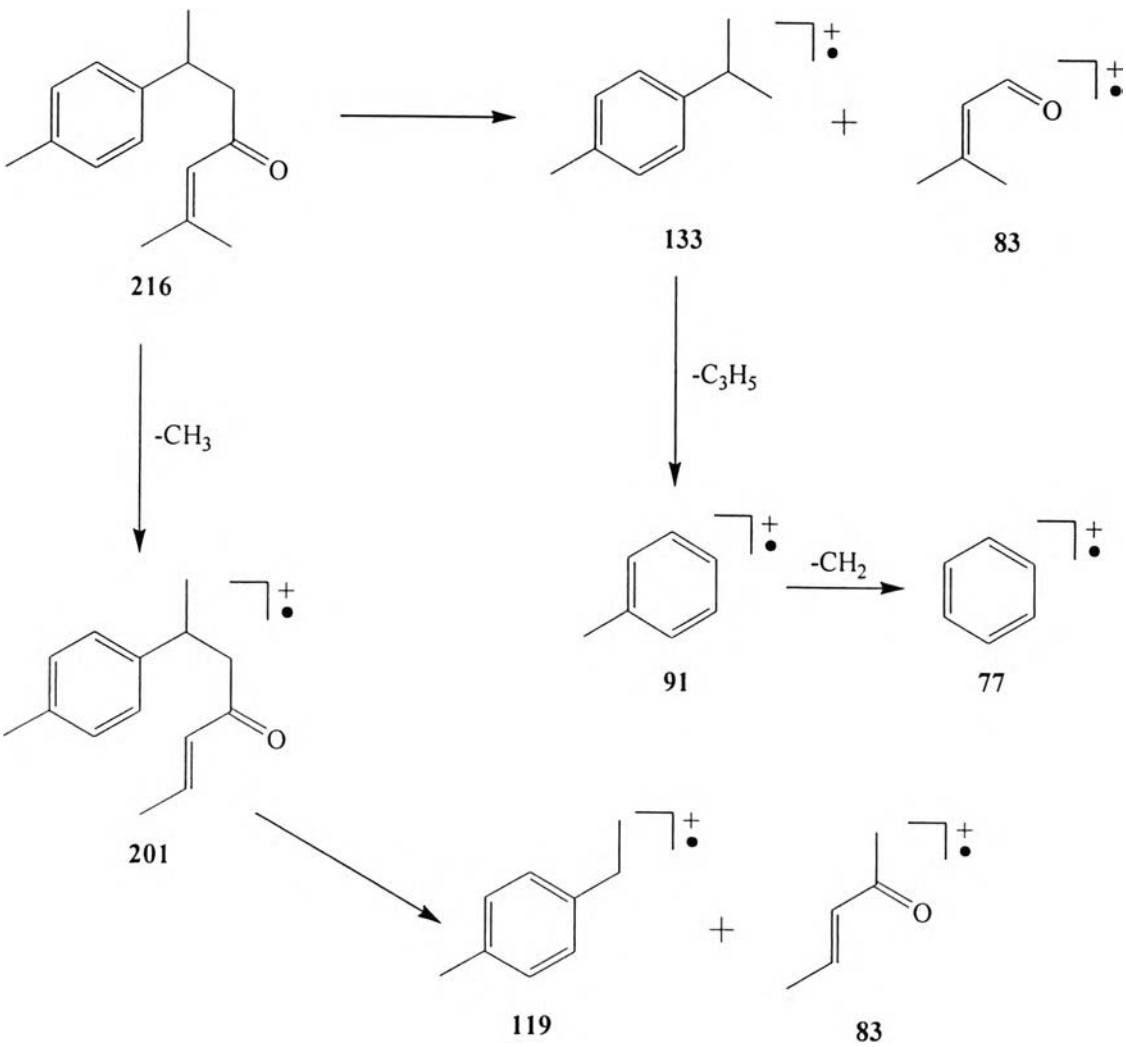

Scheme 3.4 The possible mass fragmentation pattern of Compound **4**

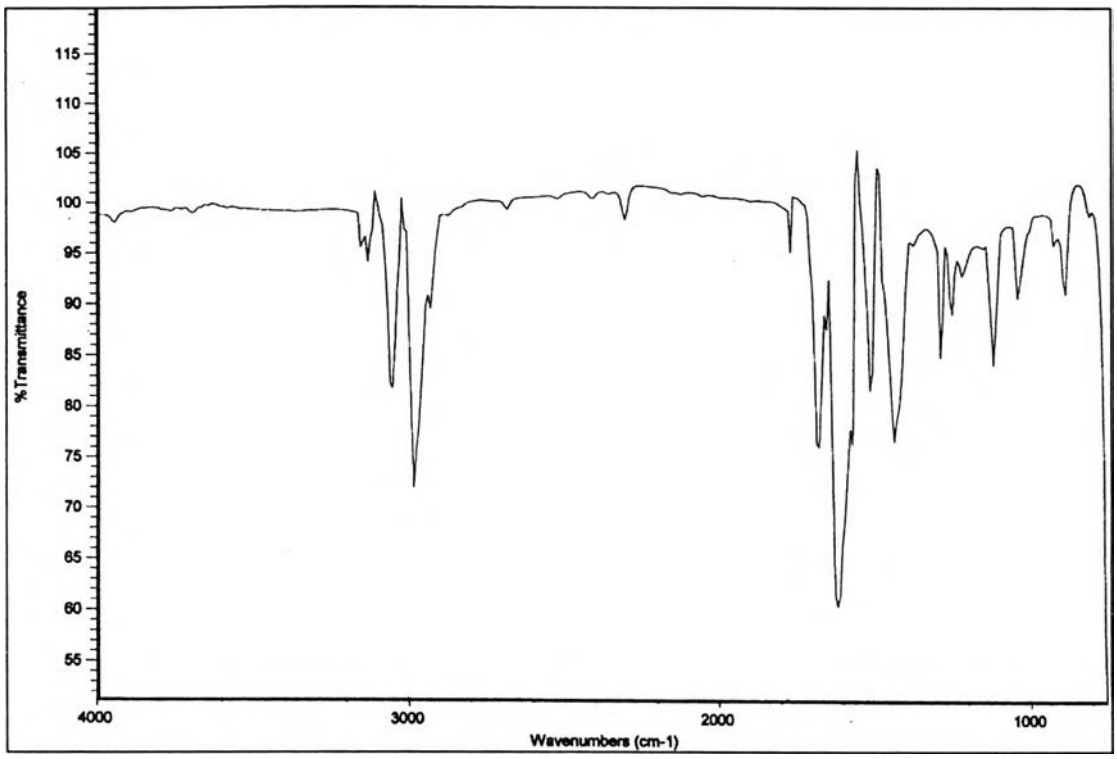

Figure 3.27 The IR spectrum of Compound **4**

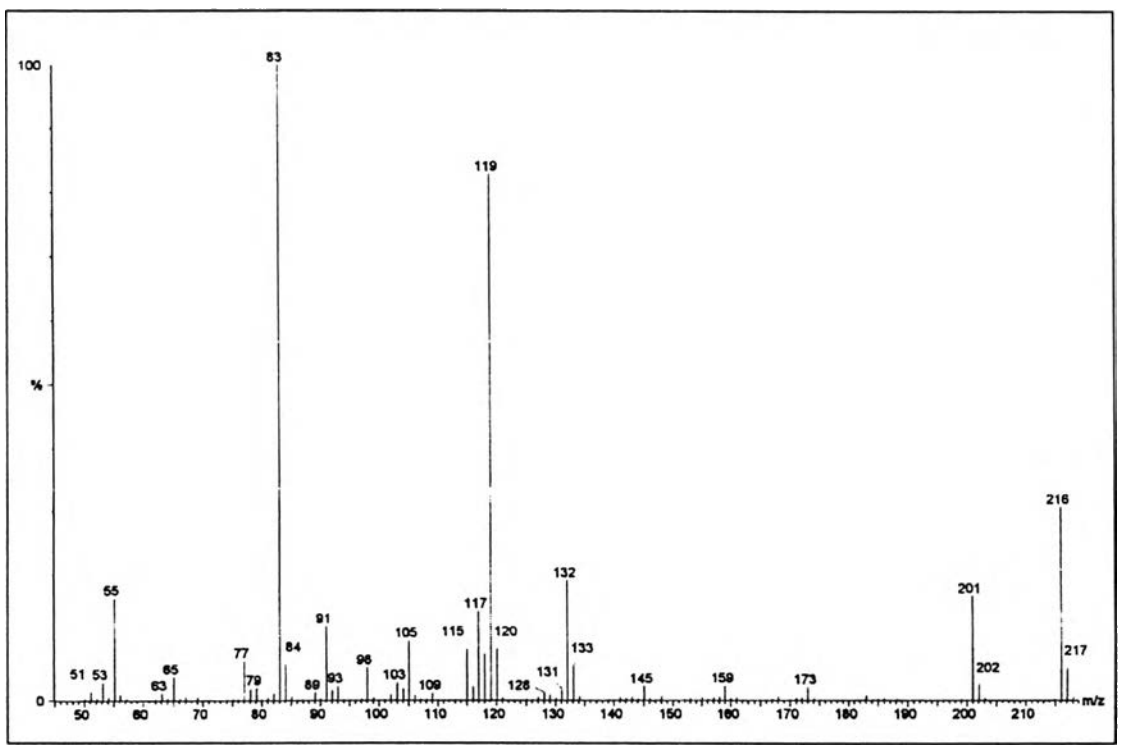

Figure 3.28 The mass spectrum of Compound **4**

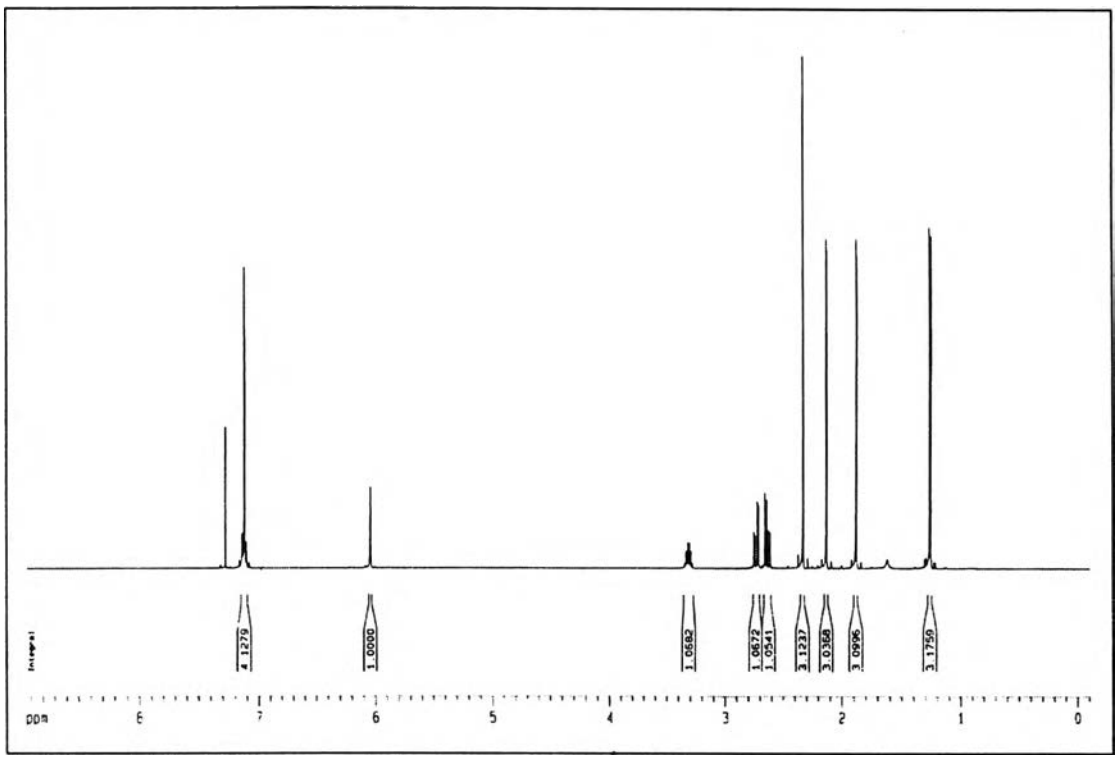

Figure 3.29 The ^{1}H NMR spectrum ($CDCl_3$) of Compound **4**

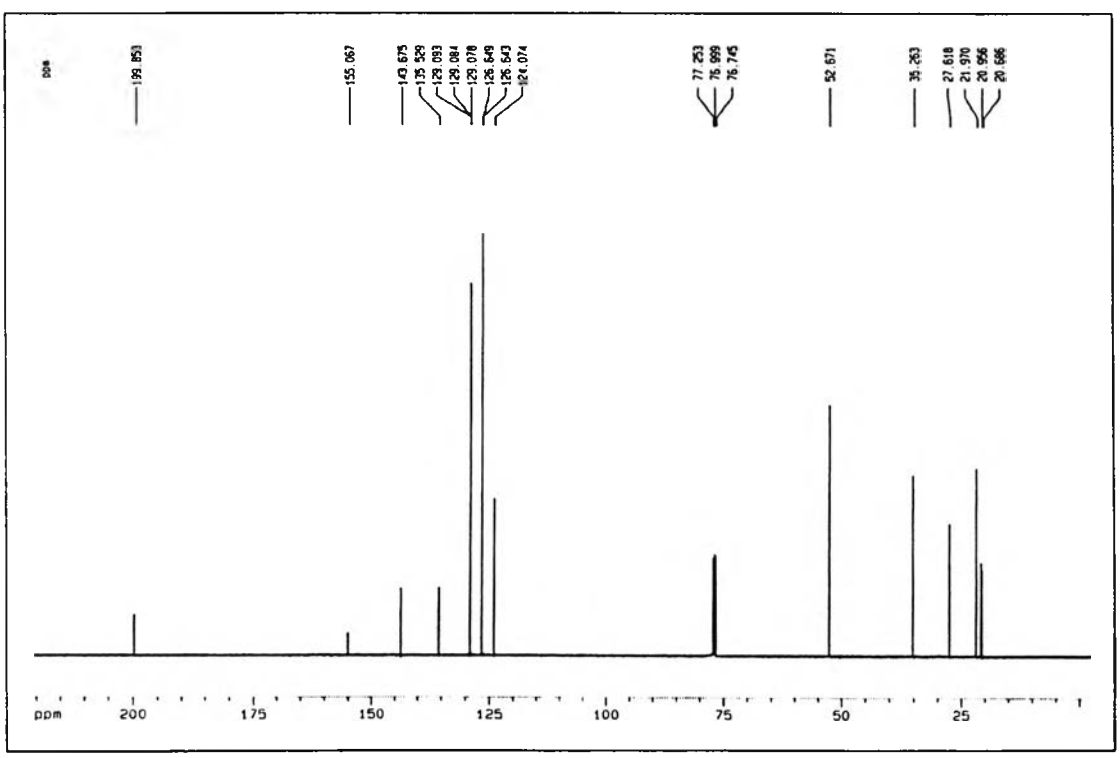

Figure 3.30 The ^{13}C NMR spectrum ($CDCl_3$) of Compound **4**

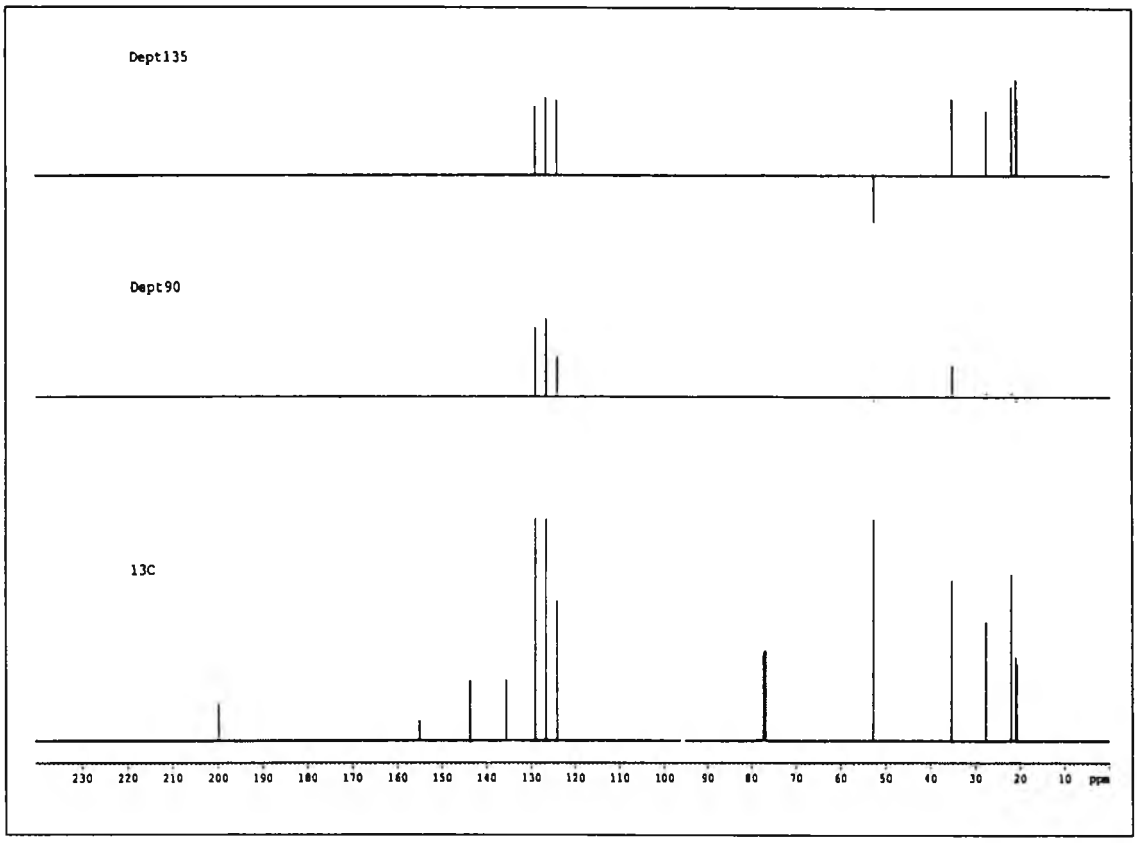

Figure 3.31 The DEPT 90 and 135 spectra of Compound **4**

3.3.5 Structural elucidation of Compound 5

Light yellow liquid (52.8 mg, 0.2 % w/w) of Compound **5** was obtained from the ethyl acetate crude extract. It was purified by chromatotron eluting with 1:9 EtOAc/Hexane. Its R_f value was 0.45 (SiO_2, $CHCl_3$).

The IR spectrum (**Figure 3.37**) exhibited the characteristic absorption band of OH stretching of hydroxy group at ν_{max} 3457 cm^{-1}, CH stretching of CH_2 and CH_3 at ν_{max} 2955 cm^{-1}, C=O stretching of ester at ν_{max} 1716 cm^{-1}, C-O stretching of ester at ν_{max} 1358 and 1214 cm^{-1}, and finally C-O stretching of alcohol at ν_{max} 1173 cm^{-1}.

Molecular ion peak of Compound **5** was at m/z 470 (**Figure 3.38**). Due to the EIMS (ion trap) technique was used, the data displayed the molecular peak of this compound.

The ^1H NMR spectrum (**Figure 3.39**) indicated the signals of four methine protons at δ 1.81 (1H, q, *J*=1.5, 2.1, 1.5 Hz), δ 2.30 (1H, m), and δ 2.81 (2H, m), eight methylene protons at δ 1.15 (1H, m), δ 1.53 (3H, m), δ 1.75 (1H, m), δ 1.81 (1H, q, *J*=1.5, 2.1, 1.5 Hz), δ 1.88 (1H, m), δ 1.97 (1H, m), δ 2.46 (3H, m), δ 2.81 (1H, m), δ 4.71 (2H, m), δ 4.85 (2H, m), and δ 4.92 (2H, m). Seven methyl protons were also observed at δ 0.84 (3H, d, *J*=6.7 Hz), δ 0.94 (3H, d, *J*=6.4 Hz), δ 1.64 (3H, q, *J*=0.9, 0.6, 0.9 Hz), δ 1.70 (3H, m), δ 1.81 (3H, q, *J*=1.5, 2.1, 1.5 Hz), and δ 2.21 (6H, q, *J*=2.1, 2.1, 2.1 Hz).

The ^{13}C NMR spectrum (**Figure 3.40**) displayed seven methyl carbons at δ 13.0, δ 13.1, δ 19.8, δ 19.9, δ 21.9, δ 23.9, and δ 24.4. Eight methylene carbons were noticed at δ 23.1, δ 26.3, δ 27.4, δ 27.5, δ 30.7, δ 33.8, δ 112.7, and δ 114.0. Its spectrum was also demonstrated four methine carbons at δ 42.7, δ 45.2, δ 52.1, and δ 56.0. Furthermore, nine quarternary carbons were also found at δ 89.6, δ 91.6, δ 120.7, δ 143.7, δ 145.3, δ 149.0, δ 149.3, δ 169.8, and δ 169.9.

From the DEPT 90 and 135 spectra (**Figure 3.41**), this compound included nine quarternary carbons, four methine carbons, eight methylene carbons, and seven methyl carbons. Considering the IR, EIMS, ^1H and ^{13} NMR, and DEPT 90, 135 data, compound **5** was assigned as $C_{29}H_{42}O_5$, showing 9 degrees of unsaturation. According to the basis of spectroscopic observation, it was inferred to be a norsesterterpene derivative.

One bond correlation (HMQC, **Figure 3.42**) and multiple bond correlation (HMBC) experiments were used to complete the structure assignment (**Table 3.11**). From the HMBC spectrum (**Figure 3.43**), in ring A, doublet signal at δ 0.84 ppm could be assigned for H-10′ (CH_3), which correlated with C-1′ (δ_C 89.6 ppm), C-5′ (δ_C 26.3 ppm) and C-6′ (δ_C 42.7 ppm), respectively. The H-9′ (δ_H 1.70 ppm) was correlated to C-3′ (δ_C 52.1 ppm) and C-8′ (δ_C 112.7 ppm). The H-8′ (δ_H 4.71 and 4.92 ppm) was related to C-3′ (δ_C 52.1 ppm). The H-3′ (δ_H 2.81 ppm) was also related with C-1′ (δ_C 89.6 ppm). On the other hand, ring B proton signal at δ 0.94 ppm could be approved for H-10″ (CH_3), which correlated to C-1″ (δ_C 91.6 ppm), C-5″ (δ_C 30.7 ppm), and C-6″ (δ_C 45.2 ppm), respectively. The H-9″ (δ_H 1.64 ppm) was correlated to C-8″ (δ_C 114.0 ppm). The H-8″ (δ_H 4.71 and 4.85 ppm) was also related to C-3″ (δ_C 56.0 ppm). However, H-3″ (δ_H 2.81 ppm) was also correlation to C-1″ (δ_C 91.6 ppm) and C-9″ (δ_C 21.9 ppm). The HMBC correlation of this compound was summarized in Figure 3.34.

In addition, the observation of the correlations between H-4′with 5′, H-4″ with 5″, H_{2a} with H_{3a} and H_{2b} with H_{3b} in the ^1H-^1H COSY spectrum (**Figure 3.44**). This relative was summarized in Figure 3.35. Moreover, ^{13}C NMR spectrum as well as the observation of the correlations in HMQC and HMBC spectrums combined with the ^1H-^1H COSY spectrum, the possible structure of compound **5** could be deduced as 1-hydroxy-1,2-di-(6-methyl-3isopropenyl-2-propionyloxy-1-cyclohexene)-1-propene or Propionic acid 2-[2-hydroxy-2-(3-isopropenyl-6-methyl-2propionyloxy-cyclohex-1-enyl)-1-methylvinyl]-6-isopropenyl-3-methyl-cyclohex-1-enylester (**Figure 3.36**). The assignment of ^1H and ^{13}C NMR of this compound were shown in Figure 3.32 and 3.33.

Table 3.11 ^{1}H NMR and ^{13}C NMR Data of Compound **5**

Position	δ_H (J in Hz)	δ_C	DEPT	^{1}H-^{13}C Connectivities (HMBC)
10′	0.84 (3H, d, J=6.7 Hz)	13.0	CH_3	26.3, 42.7, 89.6
10″	0.94 (3H, d, J=6.4 Hz)	13.1	CH_3	30.7, 45.2, 91.6
3b	2.21 (3H, q, J=2.1, 2.1, 2.1 Hz)	19.8	CH_3	
3a	2.21 (3H, q, J=2.1, 2.1, 2.1 Hz)	19.9	CH_3	
9″	1.64 (3H, q, J=0.9, 0.6, 0.9 Hz)	21.9	CH_3	114.0
4′	1.53 (1H, m) 1.75 (1H, m)	23.1	CH_2	
9′	1.70 (3H, m)	23.9	CH_3	52.1, 112.7
3	1.81 (3H. q, J=1.5, 2.1, 1.5 Hz)	24.4	CH_3	120.7
5′	1.15 (1H, m) 1.88 (1H, m)	26.3	CH_2	
4″	1.53 (1H, m) 1.97 (1H, m)	27.4	CH_2	
2b	2.46 (2H, m)	27.5	CH_2	
5″	1.53 (1H, m) 1.81 (3H. q, J=1.5, 2.1, 1.5 Hz)	30.7	CH_2	
2a	2.46 (1H, m) 2.81 (1H,m)	33.8	CH_2	
6′	2.30 (1H, m)	42.7	CH	
6″	1.81 (3H. q, J=1.5, 2.1, 1.5 Hz)	45.2	CH	
3′	2.81 (1H, m)	52.1	CH	89.6
3″	2.81 (1H, m)	56.0	CH	21.9, 91.6
8′	4.71 (1H, m) 4.92 (1H, m)	112.7	CH_2	52.1
8″	4.71 (1H, m) 4.85 (1H, m)	114.0	CH_2	56.0
1′		89.6	C	
1″		91.6	C	

Table 3.11 (cont.) ^{1}H NMR and ^{13}C NMR Data of Compound **5**

Position	δ_H (J in Hz)	δ_C	DEPT	^{1}H-^{13}C Connectivities (HMBC)
2		120.7	C	
7′		143.7	C	
7″		145.3	C	
2′		149.0	C	
2″		149.3	C	
1b		169.8	C	
1a		169.9	C	
1		~185.0*	C	

* Not observed

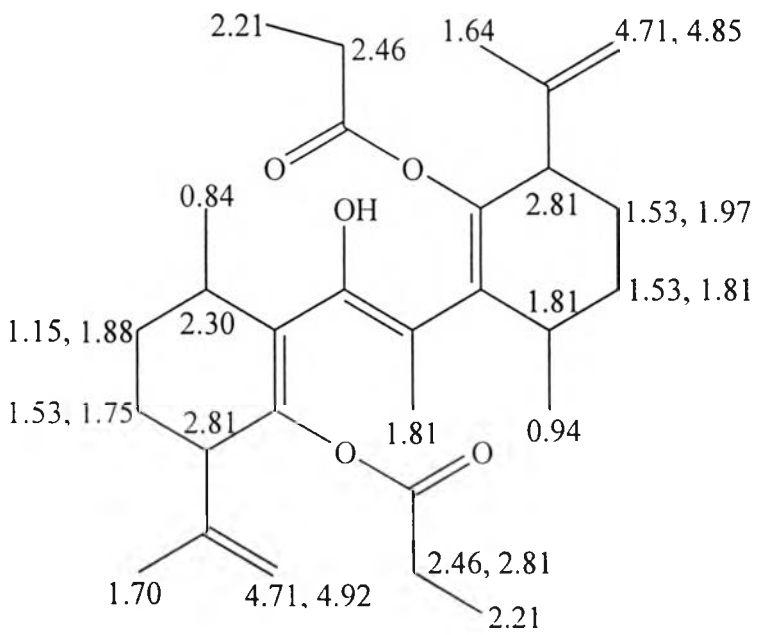

Figure 3.32 The assignment of ^{1}H NMR of Compound **5**

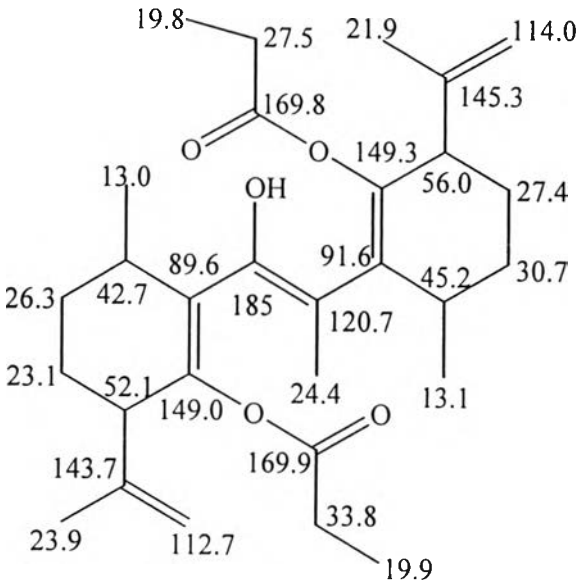

Figure 3.33 The assignment of ^{13}C NMR of Compound **5**

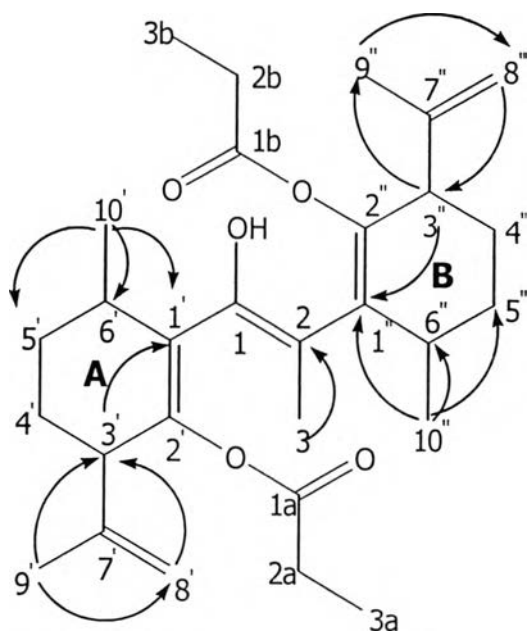

Figure 3.34 Selected HMBC correlation of Compound **5**

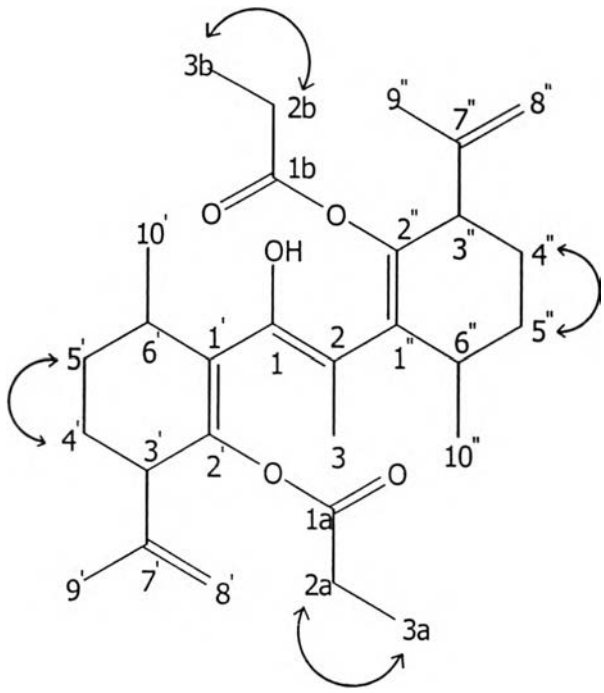

Figure 3.35 Selected COSY correlation of Compound **5**

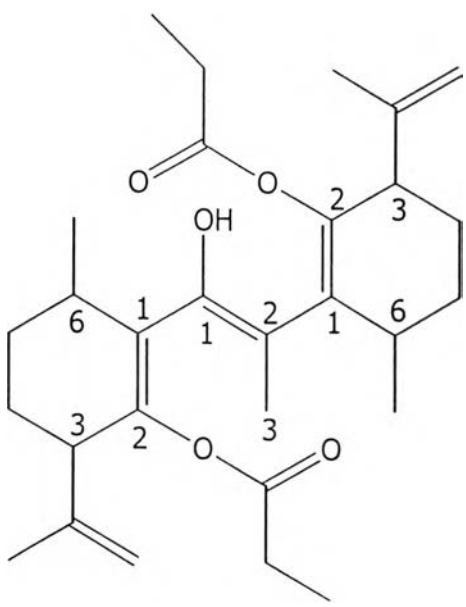

Figure 3.36 The possible structure of Compound **5** (1-Hydroxy-1,2-di-[6-methyl-3-isopropenyl-2-propionyloxy-1-cyclohexene]-1-propene)

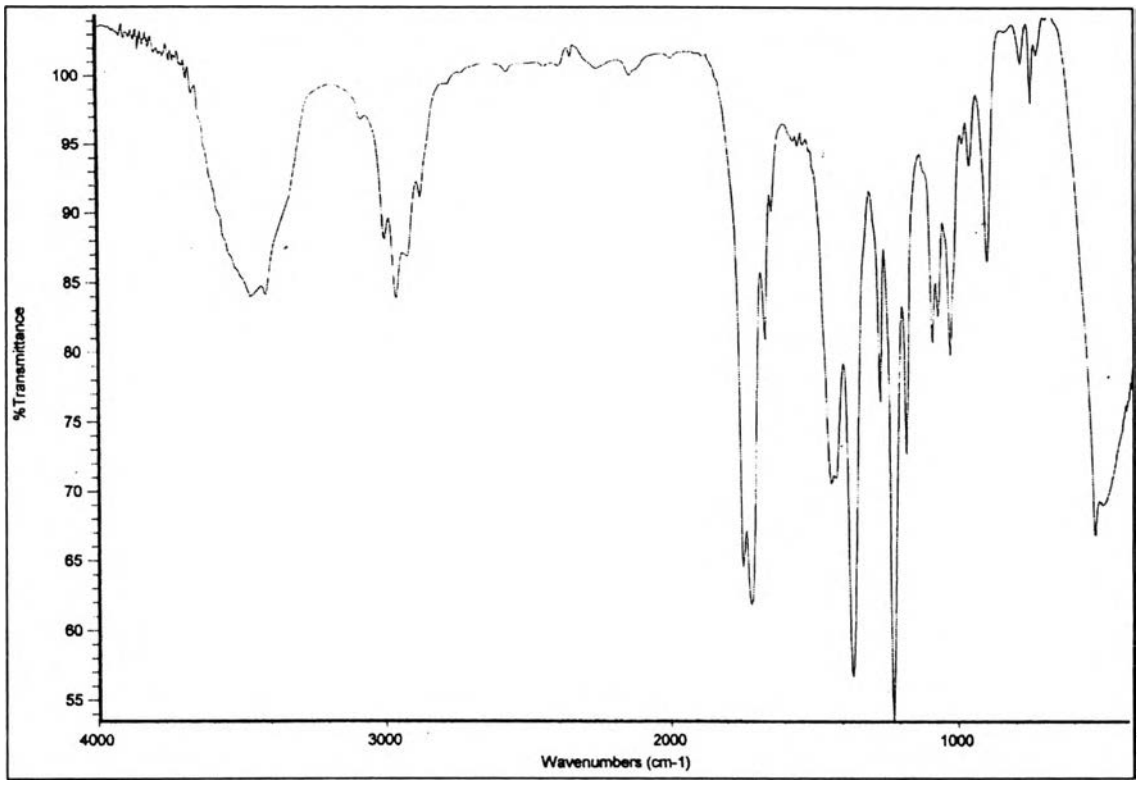

Figure 3.37 The IR spectrum of Compound **5**

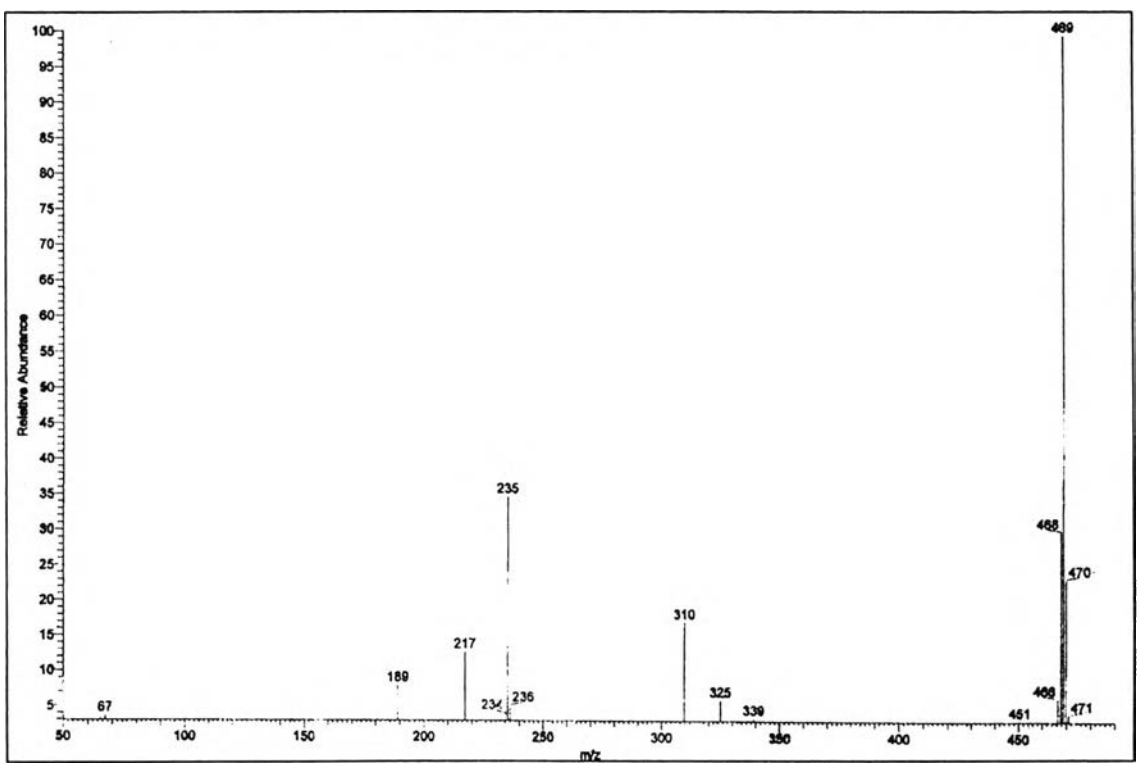

Figure 3.38 The mass spectrum of Compound **5**

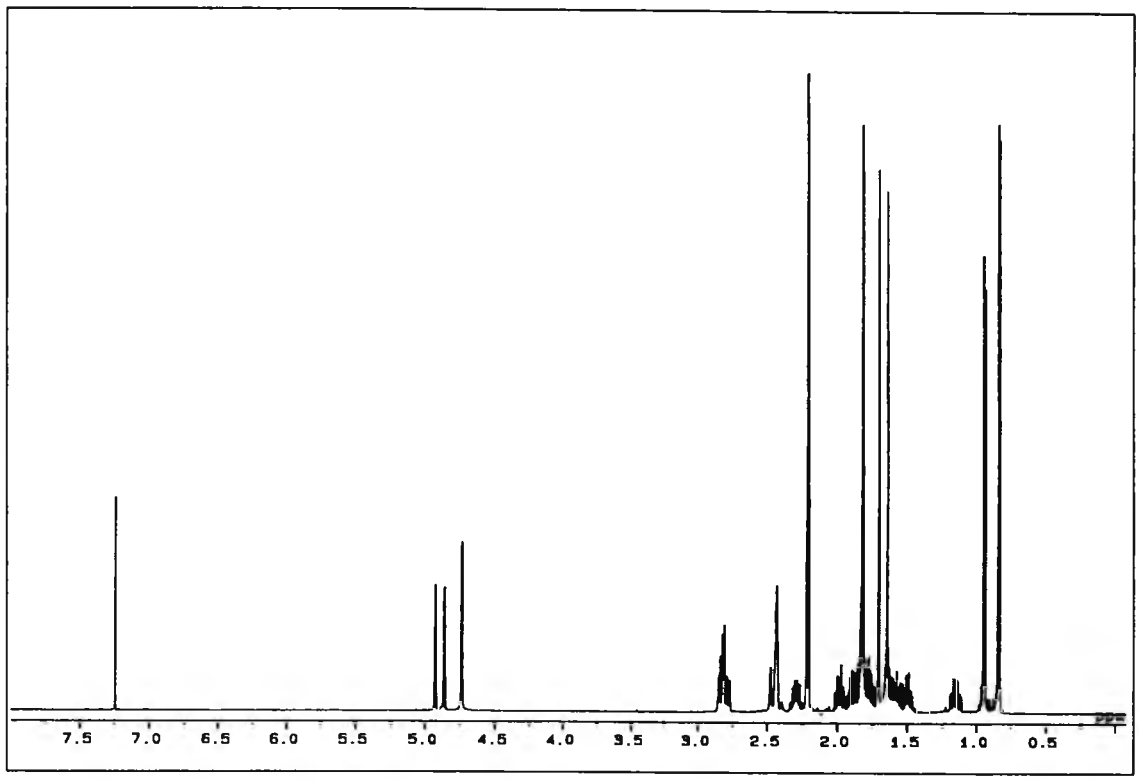

Figure 3.39 The ^{1}H NMR spectrum ($CDCl_3$) of Compound **5**

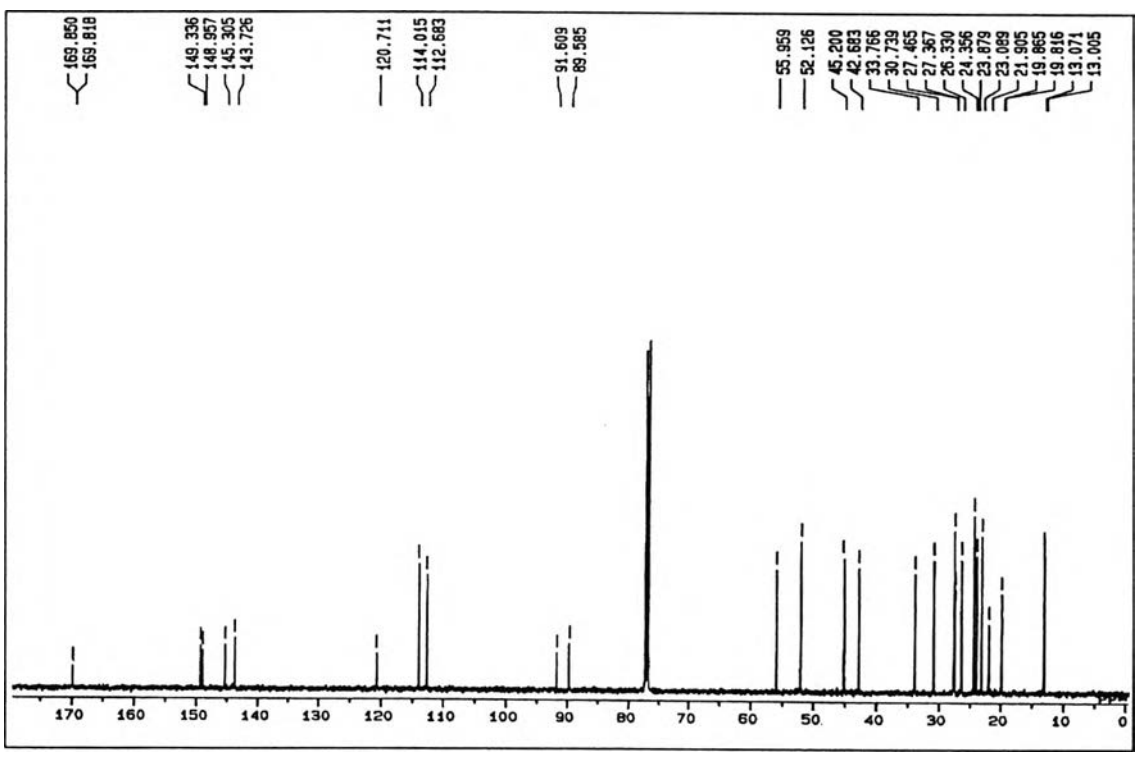

Figure 3.40 The ^{13}C NMR spectrum ($CDCl_3$) of Compound **5**

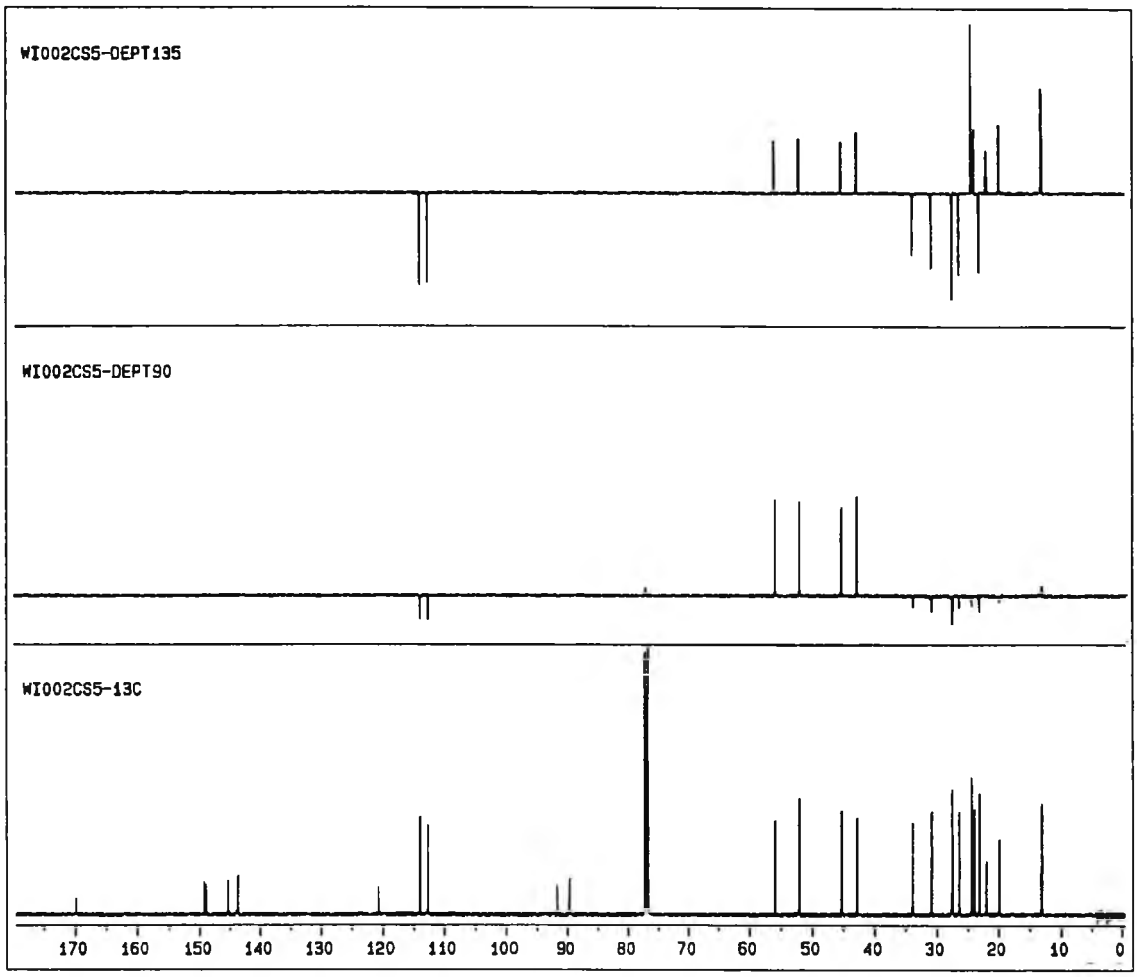

Figure 3.41 The DEPT 90 and 135 spectra of Compound **5**

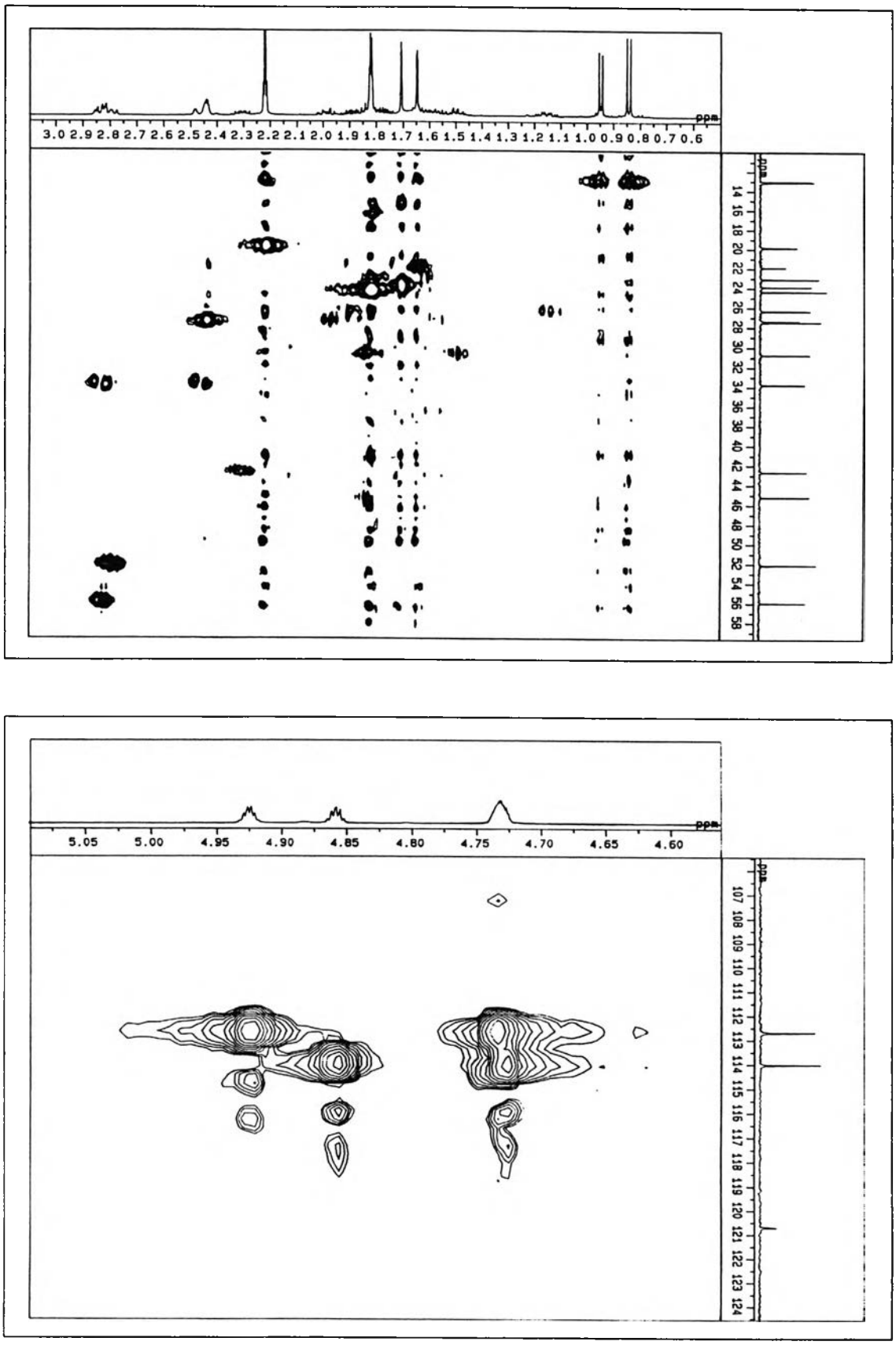

Figure 3.42 The HMQC spectrum of Compound **5**

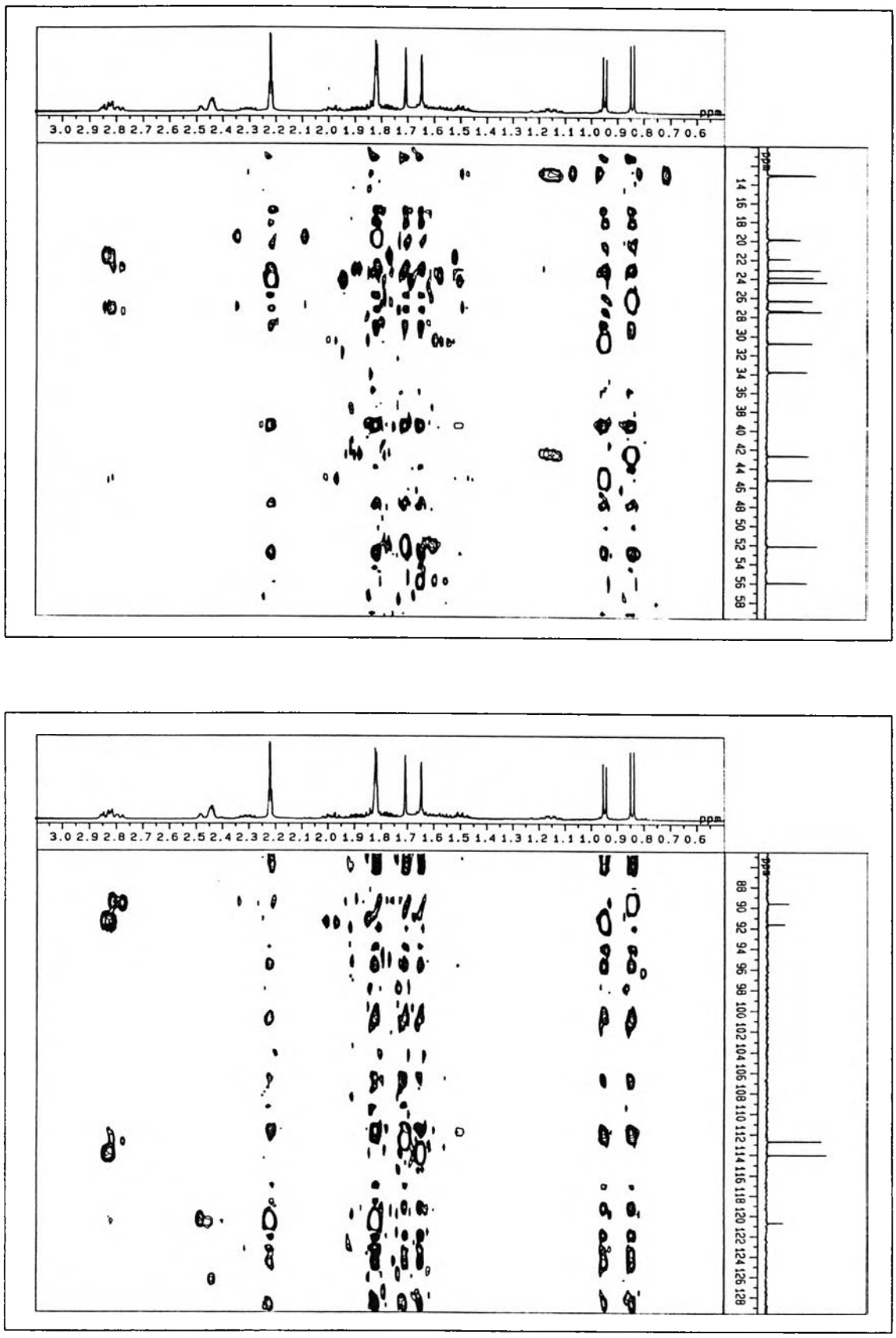

Figure 3.43 The HMBC spectrum of Compound **5**

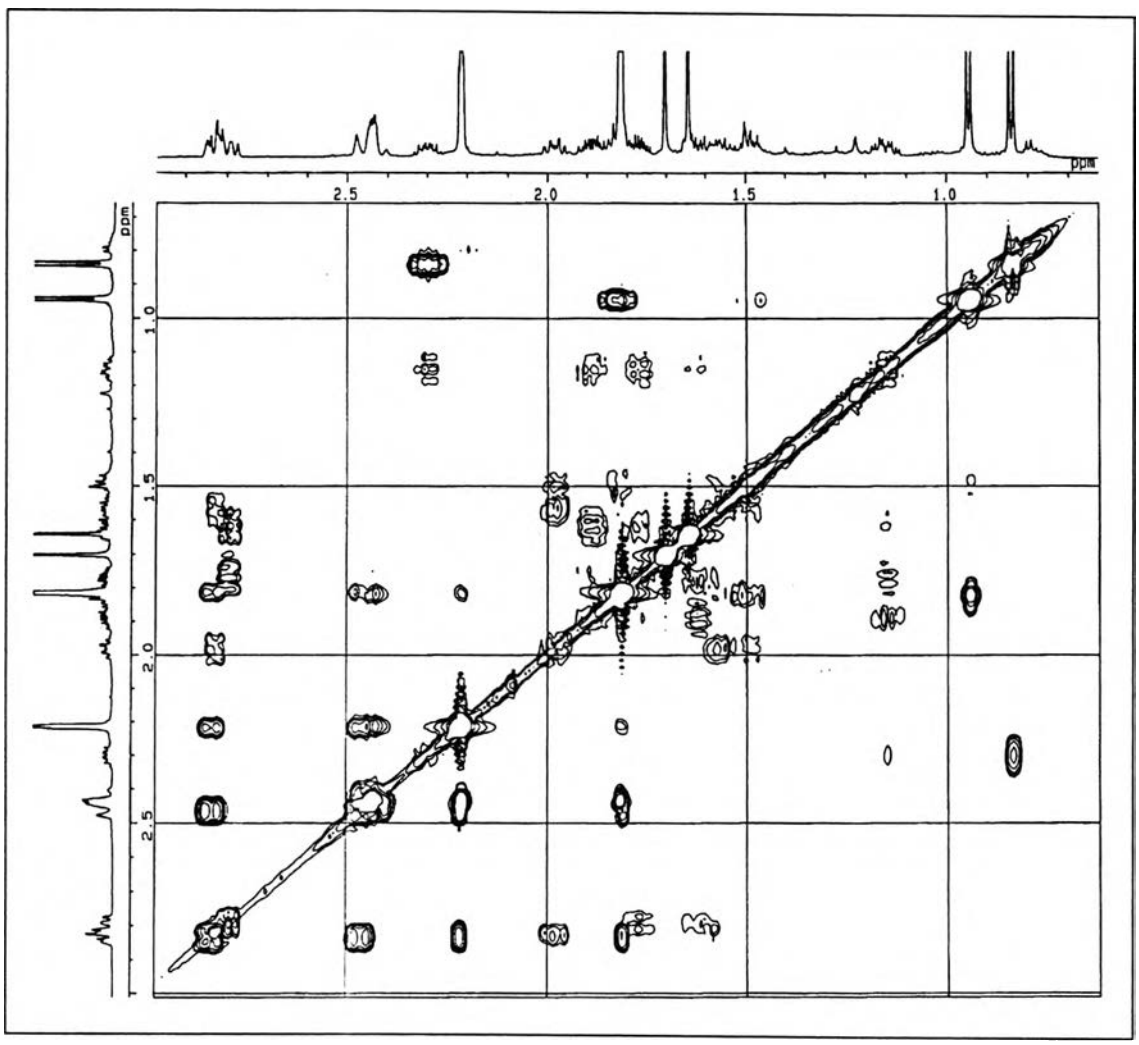

Figure 3.44 The COSY spectrum of Compound **5**

3.4 The results of antioxidant activity of isolated compounds

3.4.1 DPPH radical scavenging activity of isolated compounds

Antioxidant reacts with DPPH, which is a stable free radical, and converts it to 2,2-diphenyl-1-picryl hydrazine. The degree of discoloration indicates the scavenging potentials of the antioxidant. This research employed the TLC autographic method as a simple antioxidant assay for further isolation work. The antioxidant activity of the pure isolated compounds was measured by the spectroscopic method and compared with BHA as the reference antioxidant. These results were shown in Table 3.12, 3.13, and Figure 3.45.

The results indicated that compound **1** was found to be the most potent antioxidant (IC_{50} = 0.16 mM.). Compounds **2** (IC_{50} = 0.27 mM.), **4** (IC_{50} = 0.17 mM.), and **5** (IC_{50} = 0.19 mM.) were also highly active in the DPPH scavenging, whereas compound **3** showed the lowest activity (IC_{50} >0.50 mM.). However, these compounds exhibited slightly weaker on DPPH scavenging than that of butylated hydroxyanisole (BHA): (IC_{50}= 0.13 mM.), which was used as reference antioxidant.

Concerning the results of curcuminoids (compounds **1-3**), this evaluation was in agreement with the previous report that compound **1** has the highest activity against DPPH radical, followed by compounds **2** and **3**, respectively (Song *et. al.*, 2001). However, curcuminoids from the prior report were isolated from the ethyl acetate soluble fraction of the rhizomes of *Curcuma longa* (Turmeric). On the other hand, the scavenging effect of a mixture of compounds **1, 2,** and **3** (% Radical scavenging at maximum concentration 0.5 mM = 49.13) was weaker than that of each pure compound. It could be concluded that compounds **1**, **2**, and **3** did not have synergistic effect for scavenging free radicals.

As for compounds **4** and **5**, they were firstly isolated from Waan Ma Lueang (*Curcuma* spp.). The DPPH radical scavenging activity of these compounds was also firstly determined. The results suggested that both compounds have the reasonably activity. Therefore, compounds **4** and **5** were interesting for another scavenging activity.

Table 3.12 The percent of radical scavenging from isolated compounds compared with the commercial antioxidant as reference

Compound	Concentration (mM)	% Radical scavenging
1	5.00×10^{-1}	90.57
	2.50×10^{-1}	72.37
	1.25×10^{-1}	31.26
	0.625×10^{-1}	12.63
	0.3125×10^{-1}	3.87
2	5.00×10^{-1}	76.70
	2.50×10^{-1}	46.88
	1.25×10^{-1}	15.04
	0.625×10^{-1}	4.87
	0.3125×10^{-1}	1.68
3	5.00×10^{-1}	18.28
	2.50×10^{-1}	11.77
	1.25×10^{-1}	4.56
	0.625×10^{-1}	3.52
4	5.00×10^{-1}	72.68
	2.50×10^{-1}	58.73
	1.25×10^{-1}	45.31
	0.625×10^{-1}	26.88
	0.3125×10^{-1}	14.04
5	5.00×10^{-1}	72.41
	2.50×10^{-1}	55.73
	1.25×10^{-1}	42.31
	0.625×10^{-1}	25.70
	0.3125×10^{-1}	6.60
Mixture 1+2+3	5.00×10^{-1}	49.13
	2.50×10^{-1}	20.08
	1.25×10^{-1}	6.88
	0.625×10^{-1}	3.00
	0.3125×10^{-1}	0.50
BHA	5.00×10^{-1}	88.38
	2.50×10^{-1}	87.94
	1.25×10^{-1}	47.21
	0.625×10^{-1}	10.90
	0.3125×10^{-1}	2.43

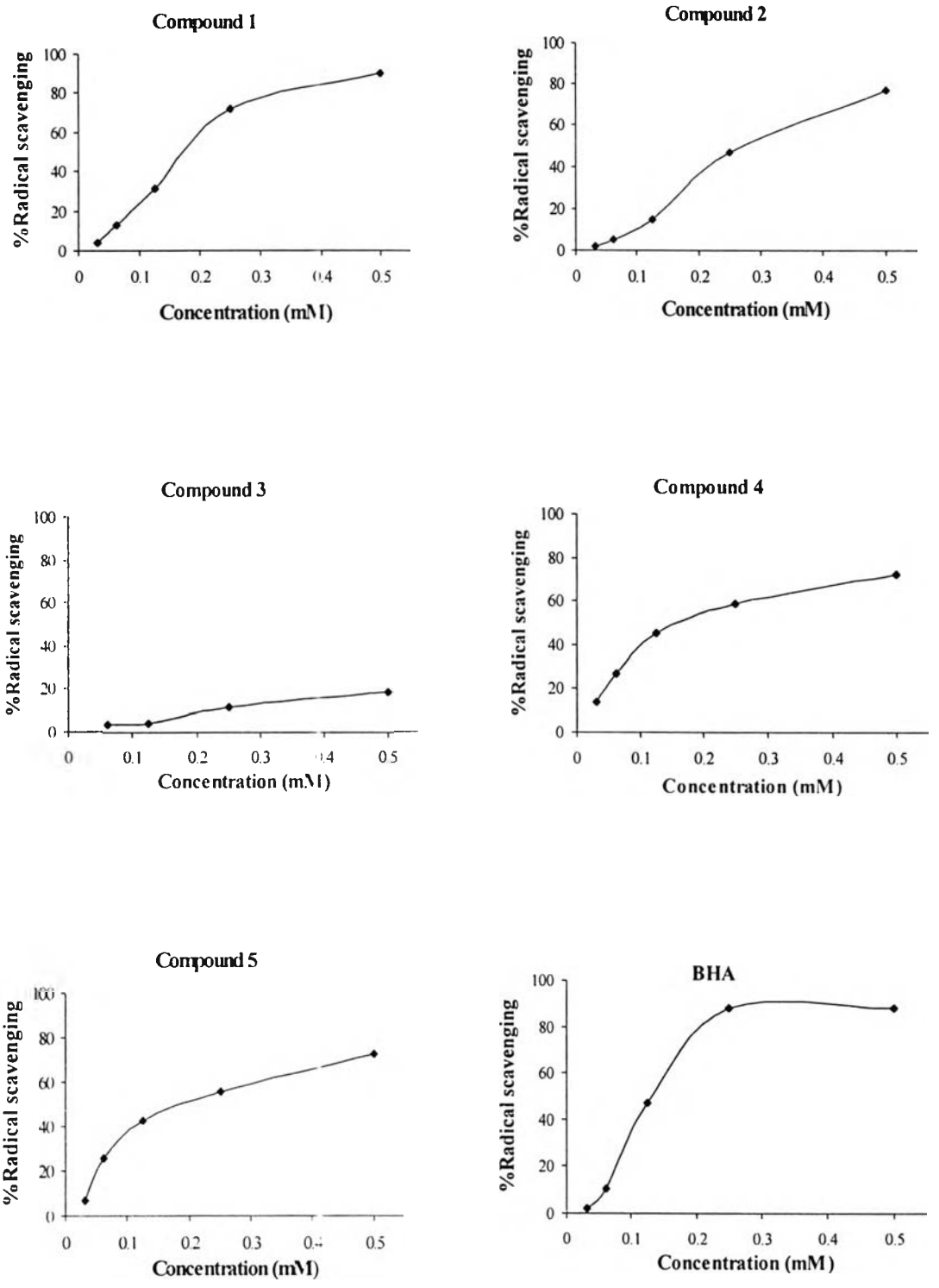

Figure 3.45 %Radical scavenging of isolated compounds compared with BHA

Table 3.13 IC_{50} of isolated compounds against DPPH radical

Compound	IC_{50}(mM)
1	0.16
2	0.27
3	>0.50
4	0.17
5	0.19
BHA	0.13

3.4.2 Xanthine oxidase-related activity of isolated compounds

(Superoxide scavenging activity and inhibitory effect on xanthine oxidase)

Xanthine oxidase is a key enzyme that catalyzes the oxidation of hypoxanthine or xanthine to uric acid. During the reoxidation of xanthine oxidase, molecular oxygen acts as an electron acceptor, generating superoxide radical and hydrogen peroxide. Therefore, xanthine oxidase is determined to be the important biological source of superoxide radicals, and inhibition of xanthine oxidase is an effectual therapeutic approach for hyperuricemia causing gout and kidney stones (Cos *et.al.*, 1998). It has been reported that the antioxidants have superoxide scavenging and inhibit xanthine oxidase activities (Nagao *et.al.*, 1999). With this viewpoint, this research evaluated both the superoxide scavenging activity using a xanthine/xanthine oxidase system and the inhibitory effect on xanthine oxidase. These results were exhibited in Table 3.14, 3.15, 3.16 and Figure 3.46, 3.47.

Table 3.14 The percent of superoxide scavenging from isolated compounds compared with the commercial antioxidant as reference

Compound	Concentration (mM)	% Superoxide scavenging
1	1.000	81.19
	0.500	64.46
	0.250	48.91
	0.125	20.15
2	1.000	78.38
	0.500	63.95
	0.250	46.33
	0.125	18.95
3	1.000	76.02
	0.500	63.08
	0.250	41.30
	0.125	21.76
4	1.000	76.19
	0.500	62.07
	0.250	48.28
	0.125	17.07
5	1.000	74.97
	0.500	61.29
	0.250	45.77
	0.125	16.58
Mixture 1+2+3	1.000	68.18
	0.500	55.38
	0.250	44.77
	0.125	28.85
BHA	1.000	83.36
	0.500	66.95
	0.250	47.22
	0.125	23.06

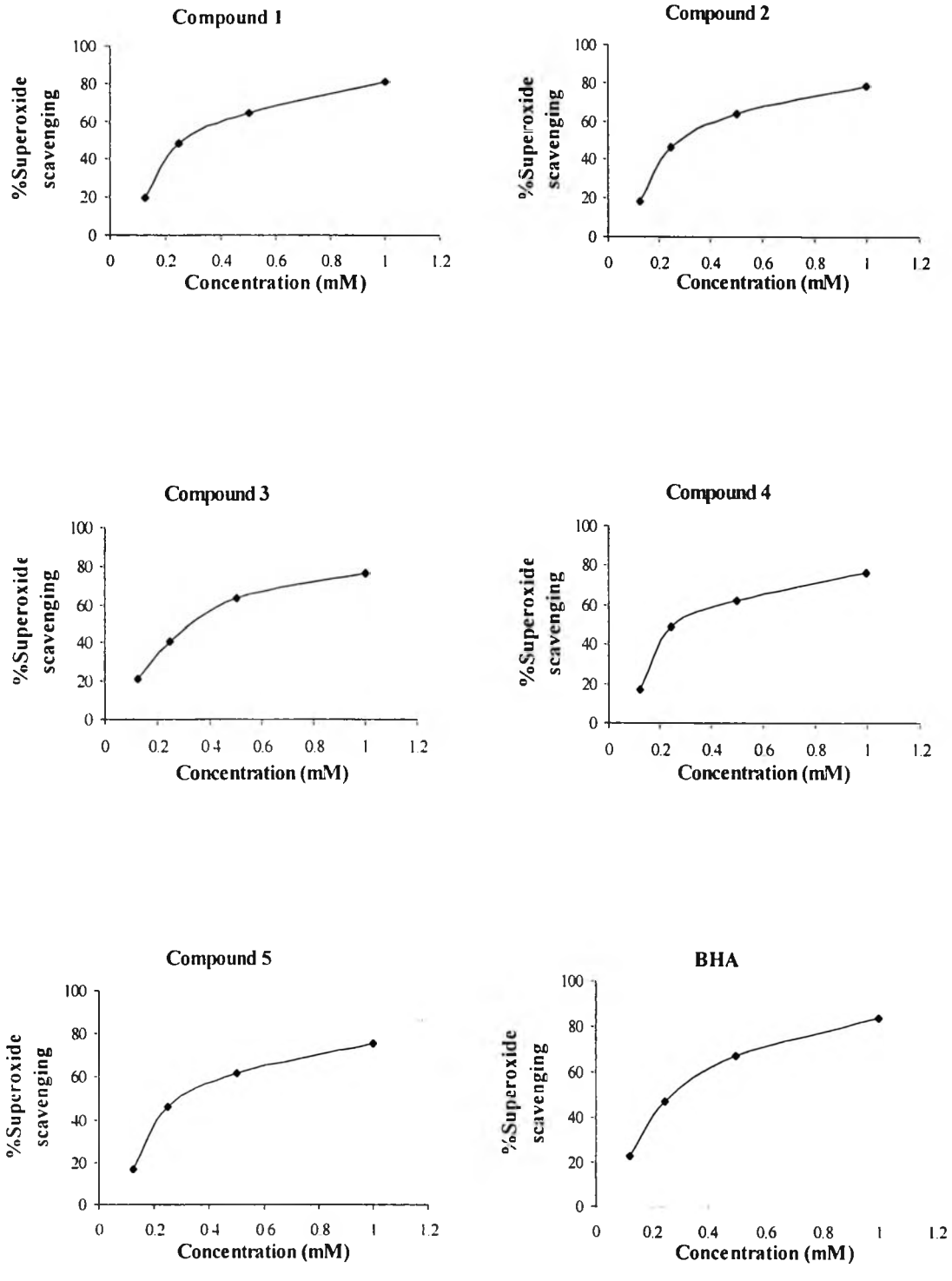

Figure 3.46 %Superoxide scavenging of isolated compounds compared with BHA

Table 3.15 The percent of inhibition and specific activity of xanthine oxidase from isolated compounds compared with allopurinol as reference compound

Compound	Concentration (mM)	% Inhibition	Specific activity* (μmole/min/mg protein)
1	1.000	82.86	0.05
	0.500	65.32	0.11
	0.250	46.87	0.16
	0.125	22.82	0.24
2	1.000	78.68	0.07
	0.500	66.25	0.10
	0.250	46.75	0.16
	0.125	22.93	0.24
3	1.000	69.02	0.10
	0.500	54.10	0.14
	0.250	42.14	0.18
	0.125	17.96	0.25
4	1.000	81.34	0.06
	0.500	66.21	0.10
	0.250	47.54	0.16
	0.125	23.14	0.24
5	1.000	80.09	0.06
	0.500	67.05	0.10
	0.250	46.96	0.16
	0.125	21.65	0.24
Mixture 1+2+3	1.000	65.71	0.11
	0.500	46.94	0.16
	0.250	27.19	0.22
	0.125	17.94	0.25
Allopurinol	1.000	81.35	0.06
	0.500	63.48	0.11
	0.250	50.20	0.15
	0.125	26.58	0.23

* Xanthine oxidase Grade III; butter milk from Sigma: 5 units/0.22 mL, which has 23 mg protein/mL.

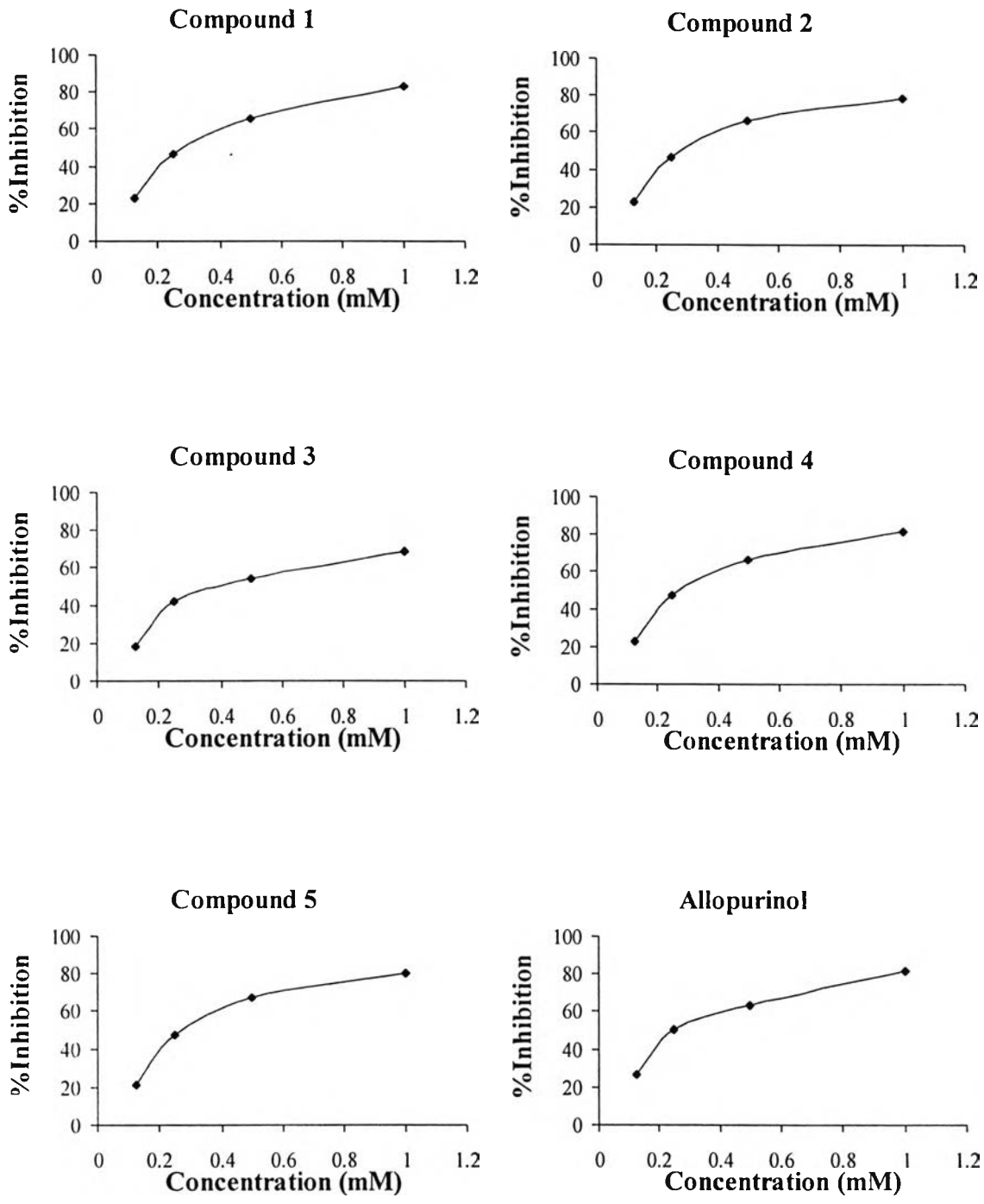

Figure 3.47 %Inhibition against xanthine oxidase of isolated compounds compared with Allopurinol

Table 3.16 IC_{50} of isolated compounds against Xanthine oxidase-related activity

Compound	IC_{50}(mM)	
	Superoxide scavenging	**Inhibitory effect on xanthine oxidase**
1	0.31	0.30
2	0.33	0.31
3	0.35	0.42
4	0.34	0.30
5	0.36	0.31
BHA	0.30	-
Allopurinol	-	0.25

Upon the results in Table 3.16, IC_{50} values of superoxide scavenging activity of the isolated compounds were in the order of compound **1** (0.31 mM) > compound **2** (0.33 mM) > compound **4** (0.34 mM) > compound **3** (0.35 mM) > compound **5** (0.36 mM). Compound **1** showed the strongest superoxide scavenging activity as well as the DPPH radical scavenging activity. Interestingly, IC_{50} value of compound **1** (0.31 mM) was in the vicinity with that of BHA (0.30 mM). It is speculated that compound **1** could replace BHA for superoxide scavenging activity.

Among the xanthine oxidase inhibitory compounds, compounds **1** and **4** exhibited the greatest inhibition effect (IC_{50} = 0.30 mM). While compounds **2** and **5** also showed intensely active with IC_{50} = 0.31 mM. Compound **3** (IC_{50} = 0.42 mM) had the weakest activity. Comparing with allopurinol (IC_{50} = 0.25 mM), drug for gout condition, it had the xanthine oxidase inhibitory effect better than isolated compounds. However, isolated compounds from Waan Ma Lueang (*Curcuma* spp.) stand a high chance of being an alternative treatment for gout in the future.

According to the result of a mixture of compounds 1+2+3 (68.18%: superoxide scavenging, 65.71%: inhibitory effect on xanthine oxidase at concentration 1.0 mM), it agreed with the scavenging effect on DPPH that it has weaker activity than that of each pure compound. Hence, it could be inferred that compounds **1**, **2**, and **3** did not have synergistic effect for xanthine oxidase-related activity.

3.4.3 Lipid peroxidation inhibitory activity of isolated compounds

Quantification of lipid peroxidation is essential to assess the role of oxidative injury in pathophysiological disorders. Lipid peroxidation results in the formation of highly reactive and unstable hydroperoxides. The ferric thiocyanate (FTC) assay measures the hydroperoxide directly utilizing the redox reactions with ferrous ion. Hydroperoxides are highly unstable and react readily with ferrous ion to produce ferric ions. The resulting ferric ions are detected using thiocyanate ion as the chromogen. For evaluation of the antioxidant activity of isolated compounds, the inhibition effect on the peroxidation of linoleic acid was investigated. The results were demonstrated in Table 3.17, 3.18 and Figure 3.48.

Considering the results obtained, the activity of compound **1** (IC_{50}= 0.19 mM) was the greatest, followed by compound **4** (IC_{50}= 0.21 mM), compound **2** (IC_{50}= 0.22 mM), compound **5** (IC_{50}= 0.24 mM), and compound **3** (IC_{50}= 0.27 mM), respectively. However, their activity were moderately lower than BHA (IC_{50}= 0.12 mM).

Among three curcuminoids, the achieved results were similar to prior assay models. Furthermore, the arrangement of their activity was also related to the result that previously reported (Toda *et.al.*, 1985). In terms of antioxidant mechanism of curcuminoids against lipid peroxidation, especially curcumin, it was found two types of radical termination, which comprise the dimer formation and the formation of the coupling product between curcumin and the lipid peroxide. The formation rate of the coupling products was almost constant regardless of the curcumin concentration, whereas the rate of the dimer production was depended on its concentration. These facts suggested that the antioxidant mechanism of curcumin, which showed about 50% reduction of the oxidation, consisted mainly with the coupling products. While increasing of curcumin concentration, it showed a stronger activity and gave a larger amount of dimers in addition to the consistently produced curcumin-lipid peroxide coupling products (Masuda *et.al.*, 2002).

From the result of a mixture of compounds 1+2+3, the gained result was in the same way with two previous assay models. The percent of inhibition at maximum concentration 1.0 mM was 53.91% that weaker than that of each pure compound. Therefore, it could be deduced that compounds **1**, **2**, and **3** did not have synergistic effect for lipid peroxidation inhibitory activity.

Table 3.17 The percent of lipid peroxidation inhibitory activity from isolated compounds compared with the commercial antioxidant as reference

Compound	Concentration (mM)	%Inhibition
1	1.0000	90.77
	0.5000	72.84
	0.2500	52.38
	0.1250	40.80
	0.0625	23.87
2	1.0000	82.58
	0.5000	65.77
	0.2500	49.02
	0.1250	40.23
	0.0625	24.81
3	1.0000	81.94
	0.5000	64.95
	0.2500	47.18
	0.1250	31.71
	0.0625	16.66
4	1.0000	82.96
	0.5000	65.95
	0.2500	49.38
	0.1250	39.82
	0.0625	25.27
5	1.0000	80.55
	0.5000	62.54
	0.2500	47.52
	0.1250	38.49
	0.0625	22.68
Mixture 1+2+3	1.0000	53.91
	0.5000	41.36
	0.2500	24.18
	0.1250	14.38
	0.0625	4.97
BHA	1.0000	92.27
	0.5000	87.34
	0.2500	69.86
	0.1250	52.23
	0.0625	33.83
	0.03125	16.84

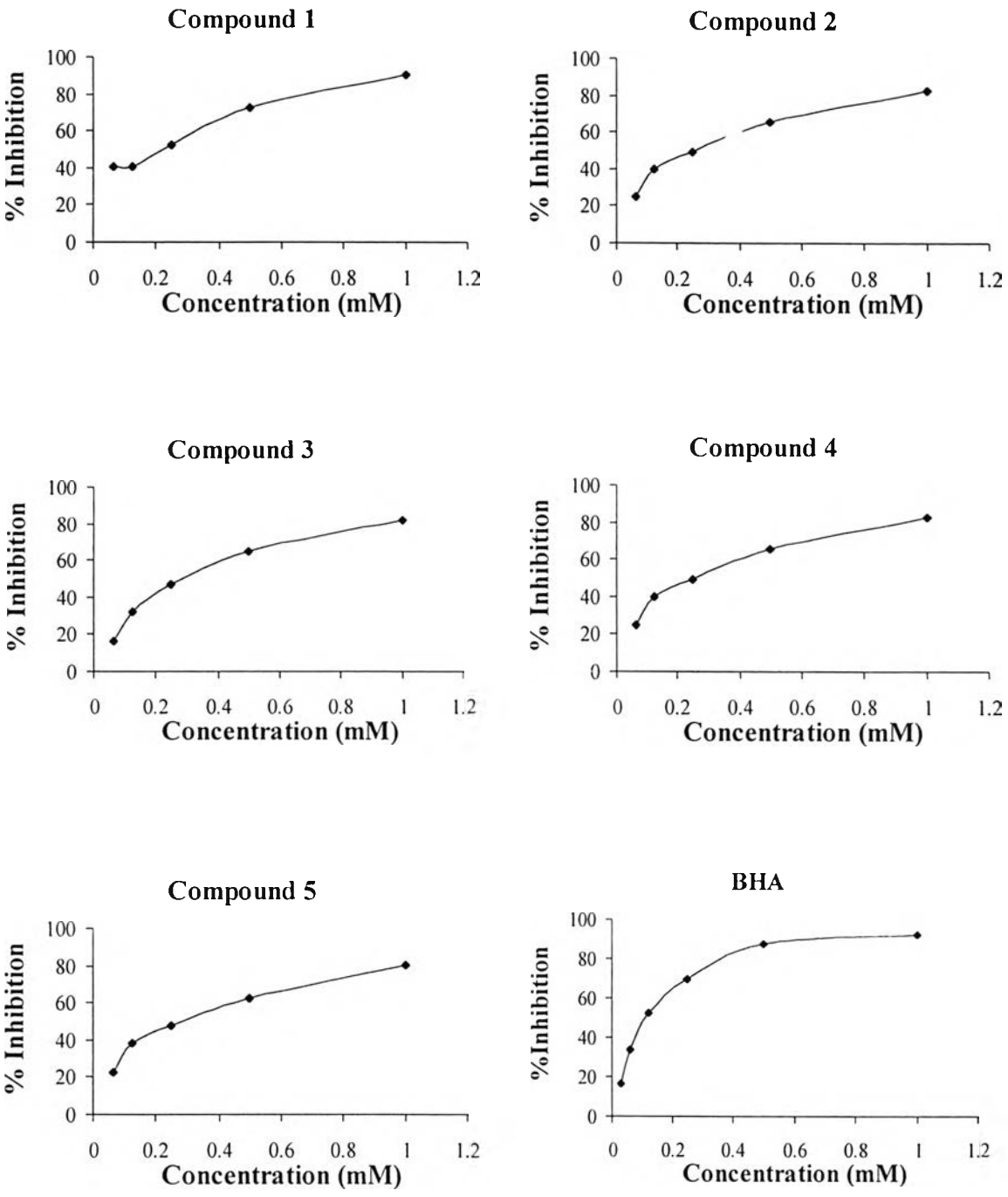

Figure 3.48 %Inhibition against lipid peroxidation of isolated compounds compared with BHA

Table 3.18 IC_{50} of isolated compounds against lipid peroxidation

Compound	IC_{50}(mM)
1	0.19
2	0.22
3	0.27
4	0.21
5	0.24
BHA	0.12

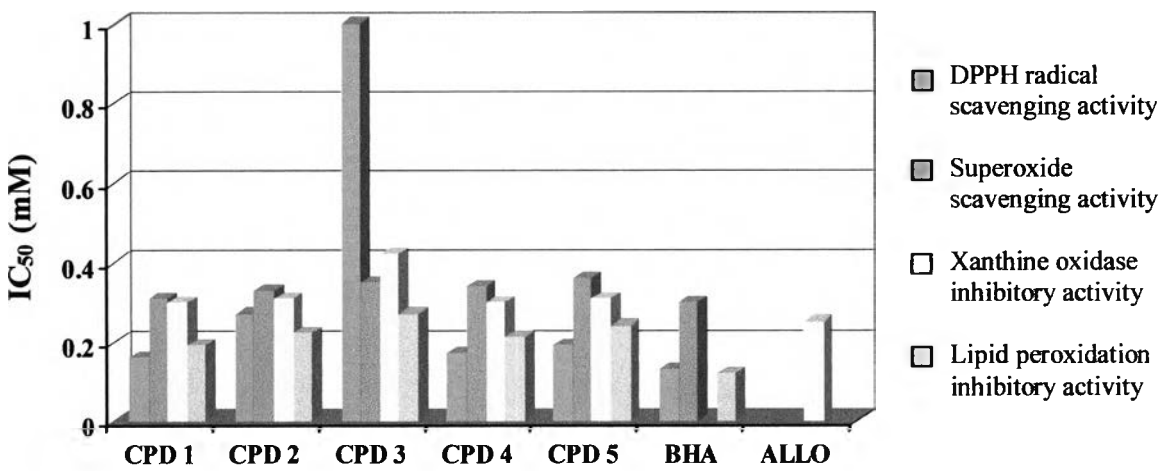

Figure 3.36 Comparison of IC_{50}values between isolated compounds and reference antioxidants from all assay models

As shown in Figure 3.49, compound 1 exhibited the strongest antioxidant activity, whereas compound 3 was found to be the weakest antioxidant. Compounds 2, 4, and 5 also demonstrated the highly antioxidant activity. In condensation, compounds 1, 2, 4, and 5 were found to be the potent antioxidants and they also had the vicinal activity. However, this research was the first report on the antioxidative components from the rhizomes of Waan Ma Lueang (*Curcuma* spp.) and all isolated compounds were also firstly evaluated for xanthine oxidase activity. Interestingly, compounds 4 and 5 were principally isolated from this plant and also discovered to be the antioxidants.

Compound **4** has been found in *Curcuma* genus: *Curcuma longa* (Helen *et.al.*, 1982), *Curcuma xanthorrhiza* (Itokawa *et.al.*, 1985), and *Curcuma zedoaria* (Hong *et.al.*, 2002). This compound has the variety of activity. It was found to be strong repellency to *Tribolium castaneum* (Helen *et.al.*, 1982). This compound also has the potent mosquitocidal activity on *Aedes aegyptii* larvae (Geoffrey *et.al.*, 1998). Additionally, this compound was retrieved to be antitumor agent for inducing apoptosis in human myeloid leukemia cells (HL-60) (Peak *et.al.*, 1996).

Compound **5** was a norsesterterpene derivative, which has the extraordinary structure. It was expected to be a new compound.